Université du Québec
à Rimouski

LES PROCESSUS SÉDIMENTAIRES DURANT LE PETIT ÂGE GLACIAIRE ET L'ACTUEL DANS L'ARCHIPEL ARCTIQUE CANADIEN

Mémoire présenté

dans le cadre du programme de maîtrise en Océanographie

en vue de l'obtention du grade de maître ès sciences

PAR

© SARAH LETAÏEF

Mai 2019

Composition du jury :

Gwenaëlle Chaillou, président du jury, UQAR-ISMER

Guillaume St-Onge, directeur de recherche, UQAR-ISMER

Jean-Carlos Montero-Serrano, codirecteur de recherche, UQAR-ISMER

France Lagroix, examinateur externe, IPGP, Paris

Dépôt initial le 19 Décembre 2018 Dépôt final le [06 Mai 2019]

Why explore? It is as well as those who ask such a question that they are others who feel the answer and never need to ask.

- Sir Wally Herbert -

REMERCIEMENTS

Je tiens tout d'abord à remercier mon directeur **Guillaume St-Onge** pour m'avoir offert l'opportunité de ce projet ainsi pour son optimisme durant ces deux années. Un grand merci à mon co-directeur **Jean-Carlos Montero-Serrano** : merci pour ton soutien, tes remarques pertinentes et les bons moments passés sur le bateau. Tu m'as beaucoup appris. Je remercie **Marie-Pier St-Onge** pour son dévouement et l'aide précieuse qu'elle a apportés à l'avancement du projet. Merci à tous les techniciens **Dominique Lavallée**, **Mathieu Babin** et **Quentin Beauvais** pour leur aide constante à la manipulation des instruments, à **Bassam Ghaleb** pour avoir répondu à mes nombreuses questions concernant les datations au plomb ainsi qu'à **Pascal Rioux** et **Christian Boutot** pour ces très bons moments passés durant les missions en mer.

Une maîtrise c'est beaucoup de temps passé au laboratoire, c'est pourquoi je voudrais aussi remercier mes collègues du labo : **Arthur Bieber**, **Julie Velle**, **Naïs Sirdeys**, **Quentin Duboc**, **Pierre-Arnaud Desiage**, **Myriam Caron**, **Simon Faye**, **Edouard Philippe** et **Charles-Edouard Deschamps** pour toutes les questions ou interrogations que j'ai pu vous posées ainsi que pour les très bons moments que l'on a partagés durant les déplacements en congrès !

Merci aussi à mes différents colocs : **Jean-François Beaudoin**, **Jordan Latour**, **Mathilde Chemel**, **Louis Landry-Massicotte** et **Pierre-Yves Francoeur** pour m'avoir fait découvrir, chacun à votre manière, la culture québécoise ! En parlant de culture québécoise, un grand merci à mes acolytes de canot à glace pour la découverte de ce sport complètement déluré et atypique qui aide à finalement apprécier le rude hiver québécois !

L'opportunité d'avoir participer à l'école d'été sur le magnétisme à Minneapolis m'a permis de rencontrer **Marco Albàn Albarran Santos**. *Gracias a ti por tu ayuda y tu comprensión. Estoy muy contenta de haberte encontrado !* L'aventure québécoise m'a également permise de rencontrer deux merveilleuses personnes : **Safwen Khamassi** et **Fatma Dhifallah**. Vous êtes vraiment géniaux, merci pour tout : les voyages à Percé, les bons repas de ramadan, les

séances de sport suivis d'une poutine et tous les « tvt » ! J'aimerais aussi te remercier **Nino** pour tout le soutien que tu m'as apporté et ces moments avec toi qui m'ont fait beaucoup de bien.

Finalement, merci à ma famille pour leur soutien, merci à mes parents qui m'ont donné le goût du voyage. Merci à ma mère pour son courage et sa ténacité. Je dédie donc ce mémoire à mes parents et particulièrement à mon père qui, je l'espère, est fier de moi, là où il se trouve.

RESUME

Les propriétés géochimiques, physiques, sédimentologiques et magnétiques de 40 échantillons de surface et de base prélevés sur des carottes boîtes dans l'Archipel arctique canadien (AAC), du plateau canadien de la mer de Beaufort vers l'est jusqu'au détroit de Lancaster (plateau/pente du Mackenzie, golfe d'Amundsen, ouest de l'Île de Banks, détroit de M'Clure, les golfes de Coronation et de la reine Maud, les détroits de Victoria, de Barrow et de Lancaster) ont été analysés afin de déterminer les processus sédimentaires récents et ceux durant le Petit âge glaciaire (PAG). Dans un premier temps, la chronologie de sept carottes a pu être établie grâce aux mesures du ^{210}Pb, où l'âge de la base des carottes est datée à ~1600 AD. Les différentes propriétés mesurées combinées à des analyses statistiques multivariées ont permis l'identification de trois provinces possédant des caractéristiques sédimentaires différentes : (1) la province de l'ouest (plateau/pente du Mackenzie, l'ouest de l'Île de Banks et le détroit de M'Clure) caractérisée par des associations géochimiques détritiques (Fe-Rb-Ti-Zn), d'important apports en matière organique, une dominance de magnétite et de minéraux magnétiques de faible coercivité et finalement un fort ratio Al/Ca (surtout durant le PAG) ; (2) la zone intermédiaire (golfe d'Amundsen et le golfe de Coronation) qui se distingue par la précipitation d'oxyhydroxydes Fe-Mn (durant la période récente), une concentration en minéraux magnétiques importante et constante ainsi qu'un mélange de matière organique d'origine marine et terrigène; (3) la province de l'est (Golfe de la reine Maud, détroit de Victoria, détroits de Barrow et de Lancaster) décrite par des apports de carbonates détritiques élevés, une matière organique d'origine marine et une prédominance de minéraux magnétique de haute coercivité ainsi qu'une augmentation de la concentration en minéraux magnétiques durant le PAG. Nos résultats confirment donc que la dynamique sédimentaire actuelle est surtout contrôlée par l'apport détritique fluviatile dans l'ouest et la zone intermédiaire alors que l'est est plus influencé par les sédiments issus de l'érosion côtière puis transportés par la glace. Les processus sédimentaires durant le PAG suggèrent une intensification de la décharge du Mackenzie, des conditions de glace et donc du transport de sédiment par celle-ci.

Mots clés : Archipel arctique canadien, Petit âge glaciaire, dynamique sédimentaire, sédimentologie, propriétés magnétiques, géochimie.

ABSTRACT

Sedimentological, geochemical, physical and magnetic properties of 40 surface and basal sediment samples of box cores collected throughout the Canadian Arctic Archipelago from the Canadian Beaufort shelf eastward to Lancaster sound (Mackenzie Shelf/Slope, Amundsen Gulf, West of Banks Island, M'Clure strait, Coronation and the Queen Maud Gulf as well as the Victoria Strait and the Barrow/Lancaster Sound) were analyzed in order to determine the modern and the Little Ice Age (LIA) sedimentary processes. Firstly, the chronology of 7 cores was established using ^{210}Pb measurements, where the base is dated on average at ~1600 AD. The different properties combined with multivariate statistical analyses have resulted in the identification of three provinces with distinct sedimentary characteristics during both periods: (1) The West province (Mackenzie Shelf/Slope, the West Banks Island and the M'Clure Strait) typified by detrital associations (Fe-Rb-Ti-Zn), important organic matter inputs, dominance of magnetite and low coercivity minerals and higher alluminosilicate contents especially during the LIA; (2) The Intermediate Zone (Amundsen and Coronation Gulfs) distinguished by Si-Al-Zr-Sr-K-Y associations, Fe-Mn oxyhydroxyde precipitation (particularly in the recent period), constant high magnetic grain concentration and a mixture between marine and terrigenous OM; (3) The East Province (Queen Maud Gulf, Victoria Strait and the Barrow/Lancaster Sound) described by high detrital carbonate inputs, marine organic matter, a dominance of high coercivity minerals and higher magnetic concentrations especially during the LIA. Our results confirm that the recent sedimentary dynamics are controlled by sediment supplies from the river discharges in the West and Intermediate Provinces whereas the East province is more influenced by sea-ice and coastal erosion. Sedimentary processes during the LIA suggest intensification of the Mackenzie River runoff, sea ice conditions and consequently of sediment transport by this latter.

Keywords: Canadian Arctic Archipelago, Little Ice Age, sedimentary dynamics, sedimentology, magnetic properties, geochemistry.

TABLE DES MATIERES

LISTE DES TABLEAUX

LISTE DES FIGURES

LISTE DES ABREVIATIONS, DES SIGLES ET DES ACRONYMES

AAC Archipel arctique canadien.

AF *Alternating field,* champ alternatif.

AW *Atlantic Water,* eau Atlantique.

BC *Baffin Current,* courant de Baffin.

BG *Beaufort Sea*, mer de Beaufort.

CAA *Canadian Arctic Archipelago,* Archipel arctique canadien.

CAC *Coastal Alaskan Current,* courant côtier d'Alaska.

CCGS *Coastal Canadian Guard Ship,* navire de la garde côtière canadienne.

C_{org} *Organic carbon,* carbone organique.

C_{inorg} *Inorganic carbon,* carbone inorganique.

C_{tot} *Total carbon,* carbone total.

H_c *Coercive Force,* coercivité.

H_{cr} *Remanent Coercive Force*, coercivité rémanente.

IRD *Ice Rafted Debris,* vêlage d'iceberg.

IPCC *Intergovernmental Panel on Climate Change,* comité intergouvernemental sur le changement climatique.

IRM *Isothermal Remanent Magnetization,* aimantation isothermale rémanente.

ISMER Institut des Sciences de la Mer.

IZ *Intermediate Zone,* zone intermédiaire.

k_{LF} *low field magnetic susceptibility,* susceptibilité magnétique mesurée à champ faible.

LIA *Little Ice Age,* Petit Âge Glaciaire.

MD *Multi-domain,* domaine multiple.

MDF_{NRM} *Median Destructive Field of the Natural Remanent Magnetization,* champs destructif médian de l'aimantation naturelle rémanente.

MSCL *Multi-Sensor Core Logger,* banc de mesure à senseurs multiples.

M_{rs} *Saturation Remanent Magnetization*, aimantation rémanente à saturation.

M_s *Saturation Magnetization*, aimantation à saturation.

N_{tot} *Total nitrogen,* azote total.

NRM *Natural Remanent Magnetization,* aimantation naturelle rémanente.

NWP *Northwest Passage,* passage nord-ouest.

OM *Organic matter,* matière organique.

PAG Petit Âge Glaciaire.

PCA *Principal Component Analysis,* analyse en composantes principales.

PML *Polar Mixed Layer,* couche mélangée polaire.

PSD *Pseudo-single Domain,* pseudo-mono-domaine.

PW *Pacific Water,* eau Pacifique.

SD *Single Domain,* domaine unique.

SIRM *Saturation Isothermal Remanent Magnetization,* aimantation rémanente isothermale de saturation.

UQAR Université du Québec à Rimouski.

WGC *West Greenland Current,* courant ouest groenlandais.

XCT *X-ray Computed Tomographic scanner,* radiographie à rayons X.

XRF *X-ray fluorescence spectrometry,* spectrométrie de fluorescence à rayons X.

INTRODUCTION GÉNÉRALE

Ce projet de maîtrise se concentre sur l'étude des propriétés physiques, sédimentologiques et magnétiques des sédiments de l'Arctique canadien afin de reconstituer les différents processus sédimentaires récents mais aussi ceux durant le Petit âge glaciaire L'introduction générale de ce mémoire présente la problématique globale qui constitue l'axe central du projet de recherche dans un contexte sédimentologique et paléoenvironnemental.

PROBLEMATIQUE: LE RECHAUFFEMENT CLIMATIQUE DANS L'OCEAN ARCTIQUE

C'est avec plus d'un siècle d'avance que l'explorateur norvégien Fridjof Nansen à son retour de la mission *Fram* (1893-1896), aborde pour la première fois l'influence des paramètres océanographiques de l'océan Arctique sur le climat global (Nansen, 1902). Il ne le savait pas encore, mais c'est à ce moment-là que Nansen touche du doigt l'une des principales raisons expliquant l'augmentation des expéditions scientifiques réalisées notamment dans l'Arctique canadien durant les dix dernières années (expéditions quasi annuelles de l'Amundsen depuis 2003). En effet, étant donné le contexte de réchauffement climatique actuel, il devient grandement important d'étudier ces différents paramètres impliqués afin de mieux comprendre les impacts passés mais aussi futurs sur le climat global.

En dépit de sa petite taille, l'océan Arctique est considéré comme un véritable thermostat climatique grâce à sa couverture de glace pérenne qui lui attribue un fort pouvoir d'albédo (Serreze et al., 2007). Mais, selon les modèles numériques du GIEC *(Groupe d'experts intergouvernemental sur l'évolution du climat ;* Pachauri et al., 2014) les régions polaires seraient celles qui se réchauffent le plus rapidement. Ce réchauffement se traduit notamment par une diminution du couvert de glace estival d'environ 13 % par décennie entre 1979 et 2014 (Serreze et Stroeve, 2015). Ceci va avoir des répercussions importantes sur la régulation du climat

mondial puisque la diminution de présence de glace va, de ce fait diminuer l'albédo et provoquer une boucle de rétroaction positive en permettant à l'océan d'emmagasiner davantage de chaleur (Manabe and Stouffer, 1980 ; Holland and Bitz, 2003 ; Comiso et al., 2008). En effet, les grandes variations du climat influencent de façon directe les processus sédimentaires via un changement des sources et des modes de transport des sédiments. Il devient alors important de documenter la dynamique sédimentaire des régions polaires réagissant aux variations climatiques actuelles et passées afin de mieux comprendre les possibles changements environnementaux dans le futur.

PRESENTATION DE LA ZONE D'ETUDE

L'archipel arctique canadien (AAC) est composé d'environ 36500 îles situées dans l'arctique Canadien et est considéré comme la seconde plus grande masse continentale arctique après le Groenland (Island et al., 2014). Ces nombreuses îles sont séparées par de multiples détroits, cours d'eau et chenaux. L'archipel s'étend d'est en ouest sur environ 2400 km et du nord au sud sur environ 1900 km (Island et al., 2014) où l'île d'Ellesmere (80° N, 79° O) représente la partie la plus septentrionale. Situé à l'ouest de l'archipel arctique canadien (AAC), le plateau du Mackenzie constitue une région côtière de la mer de Beaufort, appartenant aux côtes canadiennes de l'Océan Arctique (Mudie et Rochon, 2001 ; Wang et al., 2005). Il est large d'environ 100 km, bordé à l'Ouest par la pente du Mackenzie et à l'Est le golfe d'Amundsen (Fig. 1A). Le golfe d'Amundsen est, quant à lui, un large chenal de 400 km de long, 200 km de large, avec une profondeur d'eau d'environ 300 m (Stokes et al., 2005). Il a un rôle important puisqu'il permet la connexion entre sud-est de la mer de Beaufort et l'AAC. Finalement au nord de la mer de Beaufort, on retrouve le détroit de M'Clure qui représente le bras le plus à l'Est de la mer de Beaufort. Il fait environ 270 km de long et 90 km de large et constitue une voix d'entrée principale des eaux provenant du bassin canadien dans l'AAC. Le golfe de Coronation est, quant à lui, une zone de transition entre la partie Est et Ouest de l'AAC (Fig. 1A). Ce golfe fait 230 km

de long, 100 km de large et environ 150 m de profondeur (Pieńkowski et al., 2011). Les eaux arctiques de surface pénètrent dans cette zone via les détroits de Dolphin et d'Union (Ingram et Prinsenberg, 1998) où un seuil étroit va limiter l'advection des profondes de l'Atlantique (Beaudoin et al., 2004). Plus à l'est, on retrouve le passage nord-ouest qui traverse d'ouest en est les détroits de Victoria, Barrow et Lancaster (Fig. 1A). Ce chenal est l'un des principaux conduits d'exportation d'eau et de glace de mer venant de l'ouest de l'Arctique vers l'Atlantique Nord (Jones et al., 2003) avec des profondeurs bathymétriques augmentant graduellement d'ouest en est (Prinsenberg and Bennett, 1987).

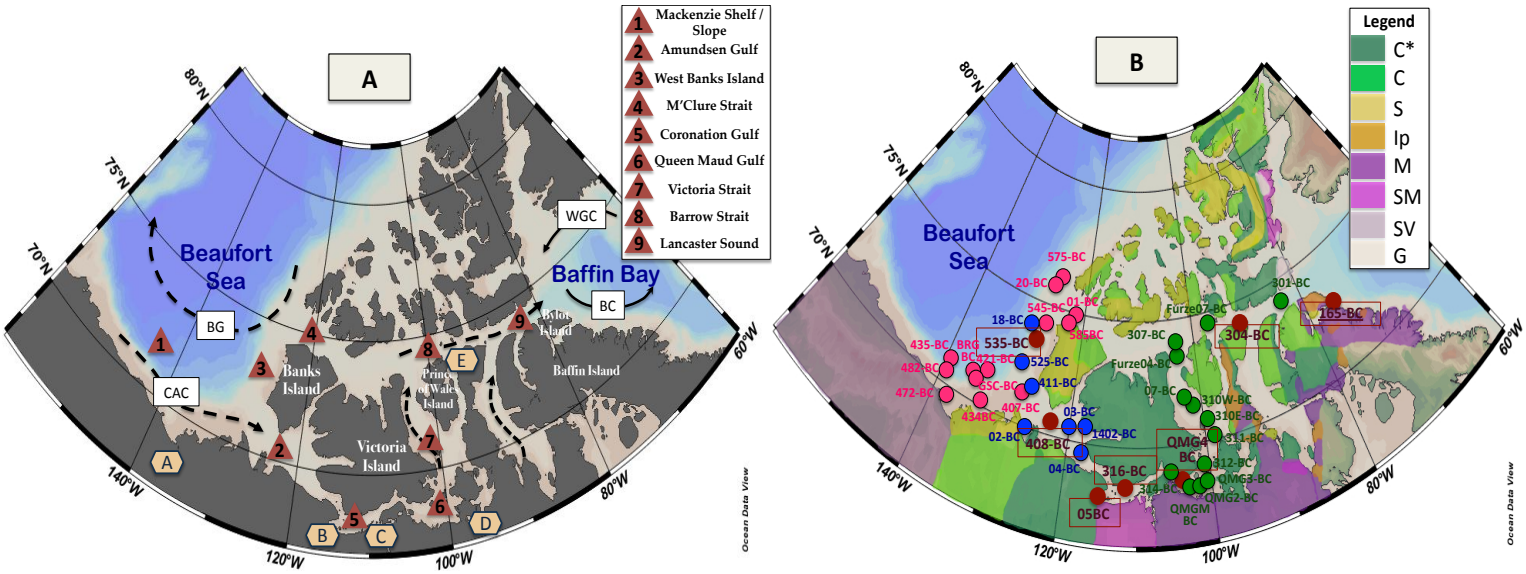

Figure 1 (A) Map of the Canadian Arctic Archipelago showing studied regions forming part of the study area. The generalized modern circulation: dashed arrows represent surface currents (BG: Beaufort Gyre and CAC: Coastal Alaskan Current) whereas solid black arrows indicate deepest Atlantic Water circulation (BC: Baffin Current and WGC: West Greenland Current). Some important rivers are also identified: A=Mackenzie River; B= Coppermine River; C= Ellice River; D= Back and Hayes Rivers and E= Cunningham River. (B) Map of the geological setting and collected dot cores. The geographic provinces discussed later in the text are also represented: pink = west; blue = intermediate zone (IZ); green = east. Framed red stations correspond to ^{210}Pb dated cores. Simplified geological units map of the CAA inspired from wheeler et al (1996), Harrison et al (2011) and modified from Alkire et al (2017). The color code represents the dominant facies: C*= dominant carbonate/evaporite; C = major carbonate unit; S = sedimentary

facies; Ip = plutonic; M = metamorphic; SM = sedimentary and metamorphic, SV = sedimentary and volcanic; G = unknown deposit influenced by the ancient glacier coverage.

VARIATION CLIMATIQUE DANS L'ARCHIPEL ARCTIQUE CANADIEN DEPUIS LE PETIT AGE GLACIAIRE (PAG)

Dans l'Archipel arctique canadien, le PAG a été daté entre 1550 et 1850 AD (Richerol et al., 2008) et a été généralement décrit comme une période plus froide et plus sèche (Anderson et al., 2007). En effet, ce serait à ce moment que les calottes glaciaires sur les îles de Devon et d'Ellesmere auraient atteint leurs maximas en termes d'épaisseur sur toute la période de l'Holocène (ex., Koerner et Paterson, 1974; Bradley, 1990; Koerner et Fisher, 1990). Ce refroidissement a également été observé sur le plateau du Mackenzie (Richerol et al., 2008 ; Bringué et Rochon, 2012), le golfe de Coronation (Pieńkowski et al., 2011 ; 2017), sur l'Île Victoria (Peros et Gajewski, 2008; 2009), la péninsule de Boothia (LeBlanc et al., 2004; Zabenskie et Gajewski, 2007), l'Île du Prince du pays de Galles (Gajewski et Frappier, 2001), l'Île Somerset (Gajewski et al 1995), l'île Prescott (Finkelstein et Gajewski, 2007), l'Île de Baffin (Wolfe, 1996) et l'Île d'Ellesmere (Hyvärinen, 1982). D'un autre côté, cette période a aussi été marquée comme plus chaude dans les détroits de Barrow et de Lancaster (Ledu et al., 2008 ; 2010) avec des températures plus chaudes qu'actuellement. Ceci a été expliqué dans un premier temps par une transition de la phase positive à négative de l'Oscillation arctique, qui a alors induit une diminution de l'advection des eaux atlantiques et donc une intensification des apports d'eaux douces plus chaudes au sein de l'Archipel arctique canadien, mais également par le délai de réponse à un changement climatique entre l'Ouest et l'Est de l'Archipel arctique canadien, comme il a déjà été observé lors de l'Optimum climatique de l'Holocène (Kaufman et al., 2004).

Périodes climatiques	Ouest	Zone intermédiaire	Est
Petit Age Glaciaire	- Plateau du Mackenzie : 1550 - 1850 AD *(Loso, 2006)* - Pente du Mackenzie : 1560 -1820 AD *(Bringué &Rochon, 2012)* - Golfe d'Amundsen : ~ 1850 AD *(Schell, 2008)*	- Golfe de Coronation : 1680-1940 AD *(Pienkowshi, 2011)*	- Détroit de Victoria : 1500-1900 AD *(Belt, 2010)* - Lancaster Sound/Baffin: 1650-1900 AD *(Ledu., 2010)* -Devon Ice cap /Maighen/ Ellesmere : 1550-1850 AD *(Koerner, 1974, 1977 et 1990)* - Penny Ice Cap : 1810-1890 AD *(Grummet, 2001)*

Table 1 Résumé des différentes datations du PAG retrouvées dans la bibliographie

Globalement, la période actuelle et plus particulièrement la dernière décennie est considérée comme étant la période la plus chaude du dernier millénaire, particulièrement dans l'Arctique Canadien (LeBlanc et al., 2004; Smol et al., 2005; Frankeltsein et Gajewski, 2007; Peros et Gajewski, 2008). Elle a été caractérisée comme étant plus humide (Peros et Gajewski, 2009) avec une diminution de la durée et de l'extension de couverture de glace (Lotter et Bigler, 2000). En effet, durant les derniers 100 -150 ans, un réchauffement d'environ 1°C de moyenne a été notamment observé sur le plateau du Mackenzie (Richerol et al., 2008; Bringué et Rochon, 2012; Durantou et al., 2012), l'Île Victoria (Podstrike et Gajewski, 2007, Porinchu et MacDonald, 2008; Peros et Gajewski, 2008; 2009) et la péninsule de Boothia (LeBlanc et al., 2004; Zabenskie et Gajewski, 2007; Peros et Gajewski, 2009). Ces variations climatiques vont donc représenter un enjeu primordial en modifiant notamment les agents de transport et les types de processus sédimentaires au sein de la zone d'étude. Il sera donc intéressant de les comparer à la fois de façon spatiale mais aussi de façon temporelle.

PROCESSUS ET TRANSPORTS SEDIMENTAIRES

Les sédiments retrouvés dans l'Archipel arctique canadien sont pour la grande majorité détritiques. Ils sont dérivés des marges continentales alentours ayant des âges et des compositions géologiques très différentes (Fig. 2). Ces apports sédimentaires peuvent être acheminés par différents agents de transport tels que la glace de mer, les rivières, les eaux de fonte ainsi que par des panaches turbides de sédiments (Andrews et Eberl, 2012). Le plateau du Mackenzie est, pour sa part, alimenté par des apports fluviatiles détritiques dérivant de la décharge du fleuve Mackenzie. Ce dernier est la principale source de sédiment dans la mer de Beaufort canadienne (Gamboa et al., 2017) et représente le quatrième plus important fleuve de l'Arctique en termes de débit d'eau douce (~420 km^3/an ; Wagner et al., 2011), mais le premier en terme d'apports sédimentaires (~127 mT/an ; Carson et al., 1998). Les sédiments en suspension déchargés par le Mackenzie forment une plume sédimentaire qui est ensuite soumise à la variation saisonnière du couvert de glace (Barber and Hanesiak, 2004; Galley et al., 2008 ; Schell et al., 2008 ; Bringué et Rochon, 2012), aux vents et aux courants (Carmack et Macdonald, 2002).

Environ 90% des côtes bordant l'océan Arctique sont affectées par la présence de glace saisonnière ou multi-annuelle (Forbes et Taylor, 1994). La glace est un agent important dans la dynamique sédimentaire de l'océan Arctique, notamment par la formation de vêlages d'icebergs (appelés également *Ice Rafted Debris* ; Fig. 2A) qui vont emprisonnés les décharges de sédiments grossiers provenant des continents, ou encore pour les transports de sédiments (Reimnitz et al., 1992). En effet deux formes de transport par la glace ont été identifiés : celui par le frasil (nommé *suspension freezing* ; Reimnitz et al., 1992 ; Darby et al., 2011 ; Fig. 2B) ainsi que celui par les glaces d'ancrages (*anchor ice* ; Reimnitz et al., 1992 *;* Darby et al., 2003 ; 2011 ; Fig. 2C). Le premier consiste à une incorporation des sédiments fins en suspension par le frasil (glace adhérente) et requiert des zones de formation rapide de glace et peu profondes. Le second requiert quant à lui, des conditions de glace permanente et consiste à remobiliser les sédiments du fond marin. Il a également été montré que l'érosion par la glace est un facteur d'apport de

sédiment très localisé mais non négligeable dans certaines régions : cap de North Head (Rachold et al., 2000), le long de la côte alaskienne de la mer de Beaufort (Forbes et Taylor, 1994), au sud ouest de l'Île de Banks (O'Brien et al., 2006 ; Belliveau, 2007 ; Gamboa et al 2017), sur l'Île Lowther (détroit de Barrow ; St-Hilaire-Gravel et al., 2010 ; 2012), le Cap Charles Yorke (Île de Baffin ; St-Hilaire-Gravel, 2011). Ce phénomène est notamment dû à la présence de glace saisonnière sur des structures non consolidées et des falaises (Rachold et al., 2000) ainsi que la montée du niveau marin (Shaw et al., 1998).

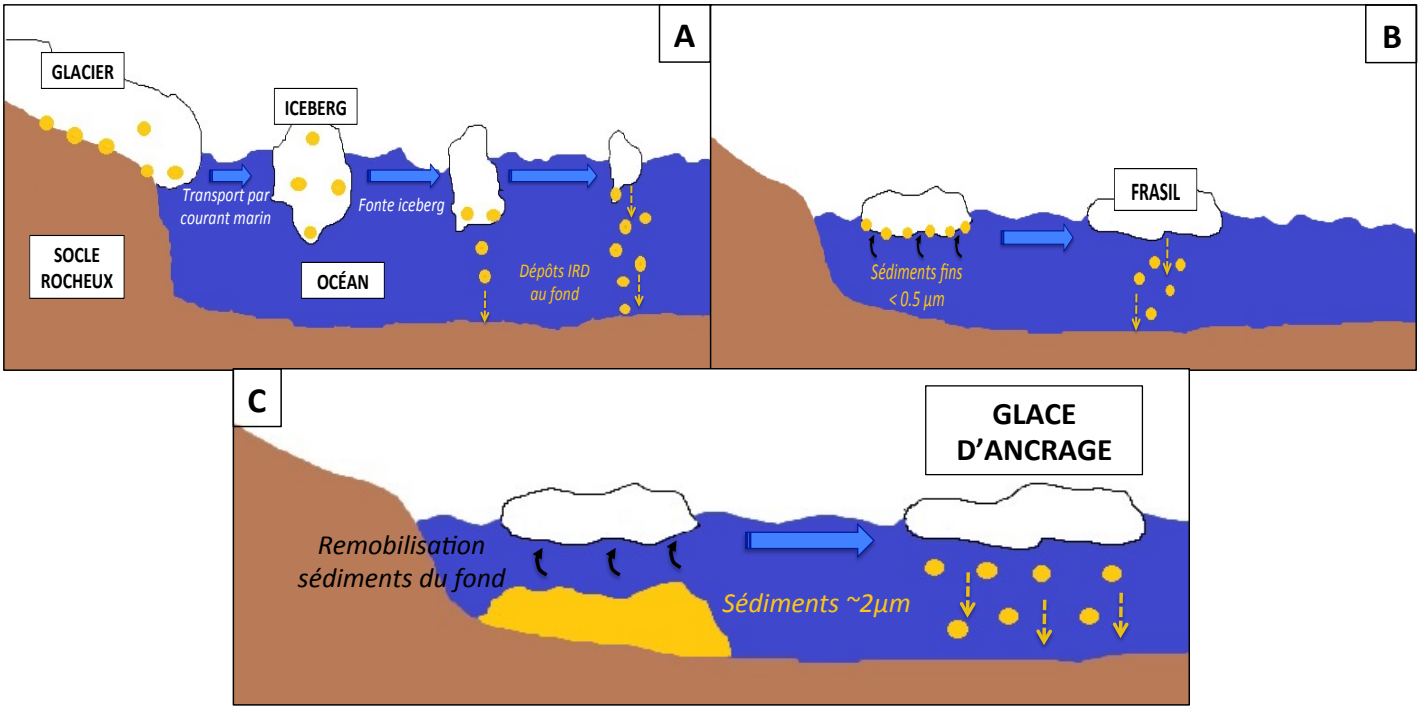

Figure 2 Représentation schématique des différents types de transport par la glace. (A) Vêlage d'iceberg. (B) Frasil. (C) Glace d'ancrage.

DEFIS ET ENJEUX POUR DATER AU ^{210}PB DES SEDIMENTS DE L'ARCTIQUE

Dans l'océan, le radio-isotope ^{210}Pb provient de la désintégration du ^{226}Ra dissous dans l'eau et de celle du radio-isotope gazeux ^{222}Rn dans l'atmosphère (Fig. 3). Le ^{222}Rn sera transformé en ^{210}Pb dans l'atmosphère pour ensuite retomber via différentes formes de précipitations. Les taux de transfert de ^{210}Pb venant de l'atmosphère sont généralement connus comme étant dépendants de la latitude (Turekian et al., 1977). En effet, la faible concentration de ^{222}Rn dans les hautes latitudes suggère une production réduite de ^{210}Pb (Hermanson, 1990), ce qui est moins représentatif de l'environnement de dépôt.

De plus, les faibles vitesses de sédimentation (Darby et al., 1997 ; Polyak et al., 2004, Belt et al., 2010 ; Bringué et Rochon, 2012) additionnées aux conditions environnementales caractéristiques de l'Arctique vont rapidement soumettre les sédiments à des processus de redistribution. Comme vu précédemment, le couvert de glace représente le principal facteur causant cette redistribution par des processus de vêlage d'icebergs (Reimnitz et al., 1992 ; Fig. 4). La présence de glace va alors affecter les transferts directs des nucléides de plomb en suspension dans l'atmosphère vers les sédiments. Par exemple, si les particules sur lesquelles le ^{210} Pb s'est adsorbé, se déposent sur la glace puis sont remobilisées par le vent ou le mouvement des glaces, les datations obtenues sont à prendre avec précautions (Nichols, 1967 ; Hermanson, 1990). Néanmoins, les processus de remobilisation par des évènements physiques, biologiques, épisodiques extrêmes, périodiques ou mêmes par érosion des sédiments fins du plateau peuvent être identifiés selon le type de profil d'excès de ^{210}Pb en fonction de la profondeur (Xu et al., 2015).

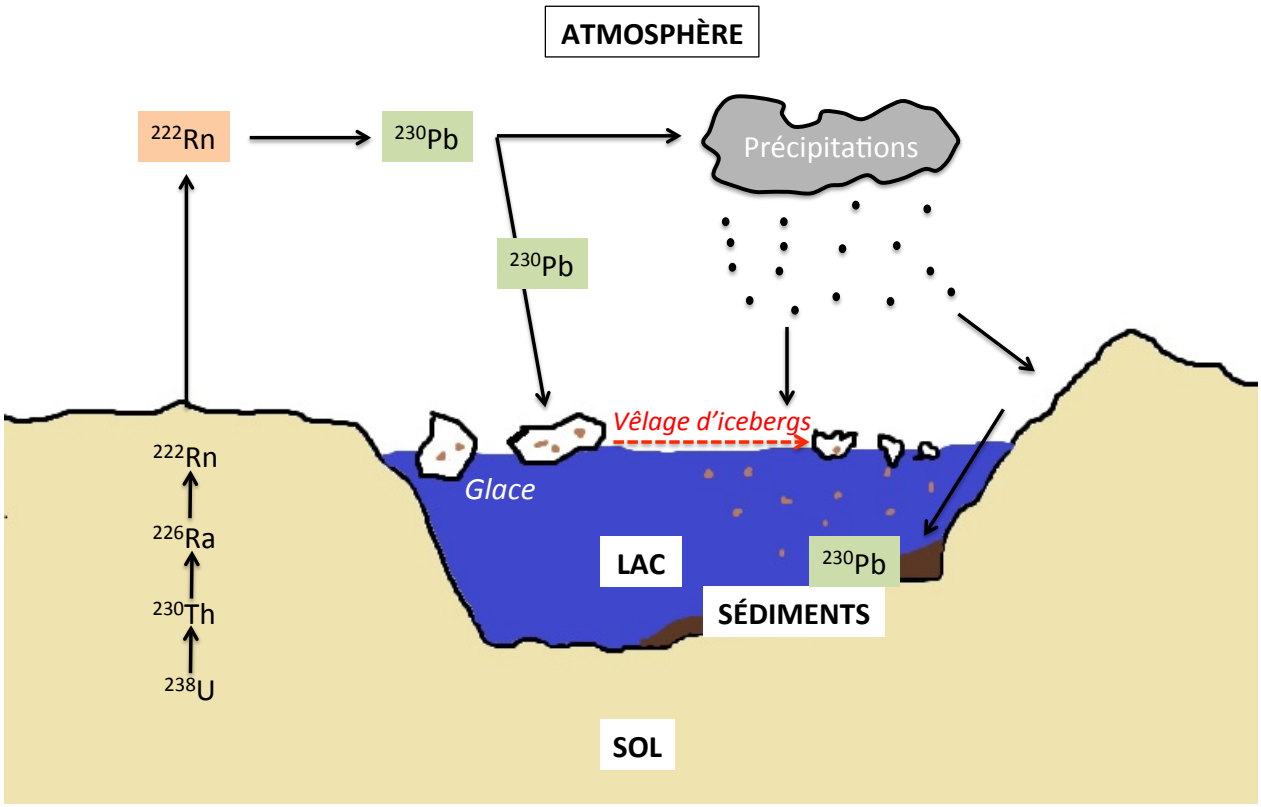

Figure 3 Cycle de formation du 210Pb. Modifiée à partir de Ghaleb et al (2017).

OBJECTIFS DE RECHERCHE

L'objectif principal de ce projet de maîtrise est de comparer les différentes propriétés des sédiments déposés durant le Petit âge glaciaire et l'actuel afin de déterminer les processus sédimentaires durant ces deux périodes de changement climatique. Des objectifs spécifiques ci-dessous ont été déterminés :

(1) Déterminer les propriétés physiques, sédimentologiques et magnétiques des sédiments de l'Archipel arctique canadien durant le Petit Age Glaciaire et l'actuel ;

(2) Déterminer et comparer les processus sédimentaires associés au Petit âge glaciaire et l'actuel.

ORGANISATION DU MEMOIRE ET CONTRIBUTION

Ce mémoire est présenté sous la forme d'un article scientifique rédigé en anglais, qui sera soumis prochainement à la revue internationale *Geochemistry, Geophysics, Geosystems* sous cette référence :

Letaïef, S., St-Onge, G., Montero-Serrano, J-C, sera soumis prochainement. Modern and Little Ice Age sedimentary processes within the Canadian Arctic Archipelago. ***Geochemistry, Geophysics, Geosystems***.

Je suis l'auteure principale de cet article qui a été rédigé sous la supervision des professeurs Guillaume St-Onge et Jean-Carlos Montero-Serrano de l'UQAR-ISMER. Je suis également responsable de la majeure partie des travaux de laboratoire à l'exception des analyses de carbone-azote élémentaires et des analyses de ^{210}Pb.

AUTRES REALISATIONS

Au cours de ma maîtrise j'ai eu la chance de présenter les principaux résultats de mon projet de recherche au cours de quatre congrès internationaux: le congrès annuel d'ArcTrain à Brèmes (Allemagne) en septembre 2017 ; *Arctic Change* à Québec en décembre 2017 ; l'*European Geoscience Union General Assembly* à Vienne (Autriche) en avril 2018 et l'*International Sedimentological Conference* à Québec en août 2018 ; ainsi qu'à deux congrès nationaux du GEOTOP (mars 2017 et 2018). J'ai également eu l'opportunité de monter à deux

reprises, à bord du NGCC Amundsen (dans l'Archipel arctique canadien en août 2017 et le golfe du Saint-Laurent en février 2018) ainsi qu'à bord du Coriolis II (dans l'estuaire et le golfe du Saint-Laurent en octobre 2016 et 2017) afin d'offrir mon aide pour les opérations de carottage, de prélèvements d'eau et de glace.

Figure 4 Photos de la mission à bord du NGCC Amundsen dans l'Archipel arctique canadien.

CHAPITRE 1

MODERN AND LITTLE ICE AGE SEDIMENTARY PROCESSES WITHIN THE CANADIAN ARCTIC ARCHIPELAGO

Sarah Letaïef, Guillaume St-Onge, Jean-Carlos Montero-Serrano

Institut des sciences de la mer de Rimouski (ISMER), Canada Research Chair in Marine Geology and GEOTOP, Université du Québec à Rimouski, Rimouski, Québec, Canada

1. Introduction

Polar regions act as the world's thermostat with their perennial ice cover and derived strong albedo. During the past decades, the Arctic region seems to be the most affected by climate warming: a decrease of 12.4% per decade of summer sea ice extent (Stroeve et al., 2011; Comiso et al., 2017) accompanied by a loss of more than 5 years old ice. Recently, less than 5% of the Arctic Ocean ice is older than 5 years old, compared to 20% in the 1980s (Serreze and Stroeve, 2015) were observed, responding to the increase of greenhouse gases emissions **(**Pachauri et al., 2014). The rapid loss of sea ice cover and thereby the albedo has played a role in amplifying Arctic warming (Holland and Bitz, 2003; Serreze and Francis, 2006; Serreze et al., 2008; Cohen et al., 2014). The magnitude of these changes around the Arctic show regional patterns and generally results in an increase in temperatures and precipitations due to an enhanced evaporation (Bintanja and Selten, 2014; Kopec et al., 2016), a northward transport of moisture (Zhang et al., 2013) and an intensification the hydrological cycle (Huntington, 2006; Peterson et al., 2006) depending on the regions.

Since the last decade, paleoclimatic studies have become more frequent for the Arctic region (Fennoscandinavia, Arctic Canada, Alaska, Greenland, etc.) using numerous proxies from

natural archives such as lakes (Gajewski, 2002; 2006; 2015), peat (Ruppel et al., 2013; Zhang et al., 2017), marine sediments (e.g., Stokes et al., 2005; Ledu et al 2010; Durantou et al., 2012, Bringué and Rochon, 2012; Pieńkowski et al., 2011; 2013; Deschamps et al., 2018 among others), ice cores (Paterson and Waddington, 1984; Mosley-Thompson et al., 2001) and tree rings (Helama and Lindholm, 2003; Linderholm and Chen, 2005; Pisaric et al., 2009). A recent review summarizes Arctic hydroclimate changes during the last two millennia (Linderholm et al., 2018) where hydroclimate simulations or proxies generally reveal that the Little Ice Age (LIA, 1550-1850 AD) tends to be drier (Ljungqvist et al., 2016) even if large regional differences are observed. During the last 2000 years, an increase in precipitation (Viau and Gajewski, 2009), river runoff (Wagner et al., 2011) and general colder reconstructed summer sea surface temperatures (e.g., Schell et al., 2008; 2009; Bringué and Rochon, 2012) has been shown in the western Canadian Arctic Archipelago (CAA), whereas a decrease in precipitation (Viau and Gajewski, 2009), an increase in sea ice cover and colder conditions were described in the eastern part (e.g., Ledu et al., 2008; 2010; Vare et al., 2009; Belt et al., 2010).

The comparisons between the different Arctic areas allow to reconstruct the climatic mosaic and the Arctic response to the ongoing global warming, but the lack of spatiotemporal analysis makes comparisons difficult. In this study, we use different proxies and a large spatial coverage of box cores from the CAA in order to compare the sediment properties from the surface (modern) and the base (LIA) of the cores to finally define sedimentary provinces and processes established during these two periods.

2. Regional settings

2.1. Regional Characteristics

The CAA is a complex array of islands covering an area of 2.9 million km^2 that represents about 20% of the total shelf area in the Arctic (Jakobsson, 2002). Narrow channels

formed by glacial erosion during the Quaternary (England et al., 2006) play an interconnecting role with larger basins. Furthermore, the Northwest Passage (NWP) connects the eastern (Baffin Bay) and western (Beaufort Sea) Canadian Arctic through the CAA. The latter is considered to be a key area for mass and heat exchanges between the Arctic and Atlantic Oceans (Melling et al., 2001, 2002; Michel et al., 2006; Dickson et al., 2007). Consequently, the export of water through the Nares and Fram Straits and the NWP will influence the formation of Atlantic deep-waters (Aagaard and Carmack, 1989, 1994) and thereby impact the global thermohaline circulation (Proshutinsky et al., 2002).

2.2. SURROUNDING GEOLOGY

The Mackenzie River drains a basin of 1.78 x 10^6 km^2 (Aziz and Burn, 2006; Hill et al., 2001). The basin is characterized, in the western part by the North American Cordillera geological unit (Mackenzie and the Rocky Mountain Belts; Millot et al., 2003) composed of sedimentary and volcanic rocks (Fig. 1B) and in the eastern part by the Canadian Shield from the Slave Province, which comprises Archean granites and gneisses (Millot et al., 2003). In turn, Banks Island is mostly composed of Cretaceous to upper Paleozoic sedimentary rocks (Fig. 1B) and Quaternary dolomite-rich tills (Bischof et al., 1996; Bischof and Darby, 2000). Otherwise, most of the islands such as, the Victoria and Prince of Wales Islands are typically underlined by Ordovician and Silurian detrital carbonates (Fig. 1B; Stokes et al., 2009). Finally, eastern Lancaster Sound is defined by Cretaceous to Plio-Pleistocene geological units associated with rifting (MacLean et al., 1990; Li et al., 2011) and Bylot Island is characterized by plutonic igneous rocks belonging to the Canadian Shield.

2.3. HYDROLOGY

Nowadays, the CAA is covered by seasonal sea ice from September to April-June (spatially variable; Vare et al., 2009; Belt et al., 2010). Likewise, because of the large

freshwater inputs (including river discharges and summer sea ice melting), the Arctic water column is strongly stratified. Typically, a cold and low salinity surface layer named the Polar Mixed Layer (PML) is found in the upper 50 to 100 m depth and is mainly formed by summer meltwaters and river discharge. The PML (Fig. 1A) is underlain by warmer and low salinity Pacific waters (PW), from 100 to 300 m depth, with a contribution of the Mackenzie River and the Yukon River waters via the coastal Alaskan current (Jones et al., 2003). Finally, a strong halocline separates the PW from the Atlantic waters (AW) until 500 to 800 m depth and enters into the system through the west Spitsbergen and west Greenland currents (Woodgate et al., 2007). Due to the presence of shallow channels generally lower than 500 m depth, the water column is predominantly composed of Pacific waters (Jones et al., 2003) coming from the Canadian Basin via the M'Clure Strait and the Amundsen Gulf. The general water mass circulation (Fig. 1A) in the CAA is strongly influenced, in the western part, by the anticyclonic Beaufort Gyre (BG) and in the central CAA by a net southeastward circulation (Ingram and Prinsenberg, 1998).

2.4. SEDIMENT DYNAMICS

The mean annual discharge of the CAA rivers was recently estimated to ~ 202 km^3/yr (Lammers et al., 2001; Alkire et al., 2017). Although the Mackenzie River discharge in the system is significant (~420 km^3/yr; Wagner et al., 2011), many CAA small rivers exist, including the Coppermine River (~88 km^3/yr), the Ellice and Back Rivers (respectively ~2.82 km^3/yr and ~15.52 km^3/yr; Déry, 2016) and finally the Cunningham River (~3.28 km^3/yr). Their individual cumulative discharge is large enough to significantly impact the freshwater flowing through the CAA and the local sedimentation.

The most important sediment entrainment in the Beaufort Sea, the Northwest Passage and globally in the Arctic Ocean is known as suspension freezing by frazil (Fig. 2B) and anchor ice (Reimnitz et al., 1993; Darby et al., 2011; Fig. 2C). Frazil consists of sediment removal by sea ice transport and requires a rapid ice formation in open and shallow water area (Reimnitz

and Barnes, 1987; Reimnitz et al., 1993). Indeed, fine-grained sediments discharged from coastal erosion or river drainages within the first 25-30 m water depth are disseminated into the first year ice during freezing storms. Then, they are transported by ice until the ice motion is stopped for the duration of winter and finally deposited elsewhere during rapid summer melting (Reimnitz et al., 1993). By using Fe-oxide fingerprinting grains, Darby et al (2003) showed that western Canadian arctic sea ice floes drift west from the Laptev Sea to Beaufort Gyre via the transpolar drift oceanic current. Furthermore, aeolian transport in the CAA was identified as insignificant and very localized (Darby et al., 1974; Reimnitz and Maurer, 1979). Furthermore, seasonal sea ice cover combined with sea ice rising, ice-rich permafrost coasts, unlithified and low cliffs promote conditions for coastal erosion (Overduin et al., 2014). For instance, the prograded beach morphology on Cape Charles Yorke (Baffin Bay) is an excellent case which show a recent sedimentary process shift from deposition to erosion, resulted from lower sediment supply, increased wave energy and sea level rising (St-Hilaire-Gravel, 2011).

3. Materials and methods

3.1. CORING AND SAMPLING

A total of 42 box cores were collected at different depths in eight different regions (Fig. 1B): the Mackenzie Shelf/Slope, the Amundsen Gulf, the M'Clure Strait, the Coronation and the Queen Maud Gulfs, the Victoria Strait and the Barrow Strait on board of the Canadian Coast Guard Ship (CCGS) Amundsen as part of the ArcticNet program in 2016 (Table 2). All coring site were targeted using high-resolution seismic profiles that indicated high sediment accumulation which are not influenced by mass wasting events (Montero-Serrano et al., 2016). In each box core, two push cores were subsampled. Using the results from digital X-ray and continuous Multi-Sensor Core Logger (MSCL) measurements processed in the lab, one replicate push core was selected for subsequent analyses based on the absence of coring disturbance/artefacts and the absence of compaction visually confirmed on deck during the sampling. In order to study the sediment-water interface, surface sediment samples were

collected on board in the uppermost 5 mm of each box core using a spatula and stored in plastic bags. Furthermore, ounces split, the cores were also sampled with 1 cm^3 cubes at the top (representing the first 1 cm) and the base (depending on the core length; Table 2) for grain-size, magnetic and sedimentological analyses.

Due to the influence of the Mackenzie River and the small Canadian Arctic rivers in the western part of the CAA (Scott et al., 2009; Belt et al., 2010; Bringué and Rochon., 2011; Durantou et al., 2012; Gamboa et al., 2017; Alkire et al., 2017) and the influence of sea ice in the eastern part of the study area (Pieńkowski et al., 2011, 2013; Ledu et al., 2010a, 2010b), the sedimentary processes that operate across the Canadian Arctic are different. As a result by using statistical analyses, sediment samples were divided into three main geographical areas (Fig. 1B): (1) West (M'Clure Strait, Banks Island Shelf and Mackenzie Shelf/Slope), Intermediate Zone (Amundsen and Coronation Gulfs), and (3) East (Central Canadian Arctic Archipelago and Northwest Passage).

Table 2 Coordinates of the studied cores. See also Figure 1.

AMD 1603 Sample Stations	Latitude (°N)	Longitude (°W)	Depth (m)	Basal Depth (cm)	Location
01-BC	74.8855	122.17016	505	40	M'Clure Strait
02-BC	70.6085	123.0285	628	39.5	Amundsen Gulf
03-BC	70.5138	120.34866	330	41.5	Amundsen Gulf
04-BC	69.6538	117.85616	415	42.5	Amundsen Gulf
05-BC	67.8645	115.07168	60	36.5	Coronation Gulf
07-BC	71.8692	102.7247	245	39.5	Victoria Strait
1402-BC	70.5463	117.6323	400	40	Amundsen Gulf
165-BC	72.7092	75.761166	645	42.5	NW Baffin Bay
18-BC	74.0076	129.127	420	44.5	West Banks Island
20-BC	75.7415	126.47666	373	27	M'Clure Strait
301-BC	74.1211	83.31972	740	38	Lancaster Sound
304-BC	74.2462	91.521966	314	45	Lancaster Sound
307-BC	74.1022	103.01421	350	37.5	Barrow Strait
310E-BC	70.8324	99.076616	216	42	Victoria Strait
310W-BC	71.4594	101.2724	163	23	Victoria Strait
311-BC	70.2809	98.5341	170	42	Victoria Strait
312-BC	69.1668	100.69713	66	45	Queen Maud Gulf
314-BC	68.9718	105.47513	89	35	Queen Maud Gulf
316-BC	68.389	112.092	182	40	Coronation Gulf
407-BC	70.0091	126.09066	390	45	Amundsen Gulf
408-BC	71.3038	127.57483	205	41	Amundsen Gulf
411-BC	71.6236	126.731	435	42.5	Amundsen Gulf
421-BC	71.3998	133.89066	1135	42	Mackenzie Slope
434-BC	70.174	133.54416	46	49	Mackenzie Shelf
435-BC	71.0768	139.6579	290	38.5	Mackenzie Slope
472-BC	69.612	138.227	124	40	Mackenzie Shelf
482-BC	70.5245	139.385	821	43	Mackenzie Shelf
525-BC	72.3924	128.95231	347	40	West Banks Island
535-BC	73.4163	128.192	289	21	West Banks Island
545-BC	74.1784	126.82341	315	39	West Banks Island
575-BC	76.1555	125.87401	318	22	M'Clure Strait
585-BC	74.5131	123.22216	382	37.5	M'Clure Strait
BRG-BC	70.9923	135.46266	664	37	Mackenzie Shelf
Furze4-BC	73.6487	103.38916	245	31.5	Victoria Strait
Furze7-BC	74.7068	97.19565	318	44	Barrow Strait
GSC-BC	70.8756	135.00083	200	38	Mackenzie Shelf
QMG2-BC	68.3164	100.80323	53	36	Queen Maud Gulf
QMG3-BC	68.3141	102.94483	56	40	Queen Maud Gulf
QMG4-BC	68.4901	103.41886	82	45	Queen Maud Gulf
QMGM-BC	68.3103	101.76546	107	41	Queen Maud Gulf

3.2. CONTINUOUS PHYSICAL AND GEOCHEMICAL ANALYSES

The whole cores were scanned with a Geotek XCT digital X-ray system at ISMER to visualize the sedimentary structures. The samples were then analyzed at 1 cm intervals with a GEOTEK MSCL to measure the physical properties, notably magnetic susceptibility (k_{LF}) and the colorimetric indices L* and a* (St-Onge et al., 2007). All the box cores were successively opened, described, photographed and analyzed again with the MSCL in the split core mode at 0.5 cm intervals. With that setting, the following parameters were determined: diffuse spectral reflectance using a Konica Minolta CM2600d spectrophotometer, magnetic susceptibility using a point source sensor and the chemical composition and concentration using an Olympus Delta Professional X-ray fluorescence (XRF) sensor. The XRF data enable to calculate geochemical ratios in order to derive more information about sedimentological processes, such as Log(Al/Ca) and Log(Mn/Al) ratios which were previously used to reconstruct the changes in sediment provenance and transport (Croudace et al., 2006; Croudace and Rothwell, 2015). Log(Al/Ca) provides a straightforward proxy to reflect sediment sources where the Aluminum can be associated to alluminosilicate inputs (Nizou et al., 2010) and Calcium to detrital carbonates. Given that Mn is highly insoluble oxyhydroxyde when oxic conditions prevail (Burdige, 1993; Calvert and Pedersen, 2007), enrichment in Mn is associated with oxic conditions. Finally, Log(Mn/Al) is used as an indicator of redox conditions (Gamboa et al., 2017).

3.3. CARBON AND NITROGEN ANALYSES

Carbon and nitrogen analyses were performed for surface and basal sediments in order to determine the spatial variations of sediment sources. The first aliquot of 6-10 mg of bulk sediment was dried, crushed and encapsulated for total carbon ($\%C_{tot}$) and total nitrogen ($\%N_{tot}$) contents. A second aliquot of 8-12 mg of sediments was acidified with 0.2 ml of HCl (1 M) to dissolve carbonates in order to measure organic carbon ($\%C_{org}$) contents. Both aliquots were analyzed using the CF-IRMS (Continuous-flow Isotope Ratio Mass

Spectrometry) coupled with a COSTECH 4010 (Costech Analytical) elemental analyzer. $\delta^{13}C_{org}$ content was analyzed in the acidified aliquot portion whereas $\delta\ ^{15}N_{tot}$ content was measured using the raw samples with a gas chromatograph coupled to a ThermoScientific Deltaplus XP mass spectrometer where the analytical error (n= 50) on measurement was 0.2 ‰ and 0.4‰ respectively. System suitability prior to analysis was evaluated using standards (caffeine, nannochloropsis and Mueller Hinton Broth). Inorganic carbon content ($\%C_{inorg}$) was calculated by subtracting the organic carbon from the total organic content. The C_{org}/N_{tot} ratio is expressed as an atomic C/N ratio and used to distinguish between marine and terrestrial sources for the sedimentary organic matter (OM; Meyers, 1994; 1997).

3.4. GRAIN SIZE ANALYSIS

Approximately 1 g of sediment was moistened with H_2O. Afterwards, 10 ml of hydrochloric acid (1M HCl) and hydrogen peroxide (30% H_2O_2) were added to remove biogenic carbonates and organic material in order to isolate the detrital fraction. Samples were then deflocculated by successive washing with distilled water and analyzed with the Beckman Coulter LS13320 laser diffraction grain-size analyzer, which has a detection range of 0.04-2000 μm. The statistical parameters (e.g., sorting, mean grain size) were computed with the GRADISTAT software (Blott and Pye., 2001) by using the method of moments in the logarithmic phi-scale.

3.5. DISCRETE MAGNETIC ANALYSES

The sampled cubes were analyzed with a 2G SRM-755 cryogenic magnetometer. The Natural Remanent Magnetization (NRM) was measured and then demagnetized at peak alternating field (AF) of 0 to 80 mT at 5 mT steps. The Anhysteretic Remanent Magnetization (ARM) was induced by an AF of 100 mT and a direct current (DC) biasing field of 0.05 mT. The Isothermal Remanent Magnetization and the Saturated Isothermal Magnetization (IRM

and SIRM) were respectively acquired using a 2G-pulse magnetizer in DC fields of 300 and 950 mT. Both ARM and IRM were then demagnetized at the same AF steps as the NRM. In the case of SIRM, the demagnetization steps were operated at 0, 5, 10, 30, 50 and 80 mT. In addition, the median destructive field (MDF) is the required field to remove half of the initial remanence and is influenced by magnetic grain size and mineralogy.

Moreover, magnetic susceptibility was also measured on some samples using a Bartington MS2E meter to determine the frequency dependent magnetic susceptibility. The difference between these two measurements is used to indicate the presence of super paramagnetic minerals (e.g., Dearing, 1999). Superparamagnetic crystals are smaller than ~0.03 μm and show rapid changes over time in their magnetic behaviour (Dearing, 1999).

Finally, sediment samples were measured using a Princeton Measurement Corporation Alternating Gradient force Magnetometer (MicroMag 2900 AGM) in order to define hysteresis loops and determine the coercivity force (H_c), the coercivity of remanence (H_{cr}), the saturation magnetization (M_S) and the saturation remanence (M_{rs}). The resulting coercivity (H_{cr}/H_c), remanence (M_{rs}/M_s) ratios and the shape of the hysteresis loops are indicative of the magnetic mineralogy and grain size (Day et al., 1977; Dunlop, 2002).

3.6. ^{210}Pb MEASUREMENTS

Recent sedimentation rates were derived from seven cores (05-BC, 165-BC, 304-BC, 316-BC, 408-BC, 535-BC and QMG4-BC) based on ^{210}Pb measurements at GEOTOP (Montréal). Approximately 2 g of dried and crushed sediment were sampled at 1 cm intervals until 15 cm and at each 5 cm until reaching the core bottom. The ^{210}Pb measurements were made after chemical treatment purification and deposition on a silver disk following routine procedures and using an EGG ORTEC model 576 alpha spectrometer. Excess ^{210}Pb measurements were processed by counting the activity of the ^{210}Po daughter isotope (Zhang, 2000) and the ^{209}Po was used as a chemical yield. The counting error was evaluated at 1σ ~ 2-4%. To estimate the sedimentation rates, we firstly visually determined the $^{210}Pb_{supported}$ and

secondly calculated the $^{210}Pb_{excess}$ ($^{210}Pb_{excess}$= ^{210}Pb- $^{210}Pb_{supported}$). Then, using the CRS model (constant rate of ^{210}Pb supply; Appleby and Oldfield, 1983; Oldfield and Appleby, 1984), the slope of the linear regression between the ln ($^{210}Pb_{ex}$) versus depth is used to calculate the average sedimentation rate (SR) = -ln (2)/(slope*22.3) where 22.3 is the half-life of ^{210} Pb (e.g., Ghaleb, 2009). This SR allows us to estimate the age of oldest sediments (base) of the measured cores.

3.7. STATISTICAL AND SPATIAL APPROACH

The geochemical data are compositional, i.e. vectors of nonnegative values subjected to a constant-sum constraint (of 100%). This implies that relevant information is usually contained in the relative magnitudes and the statistical analysis must focus on the ratios between components (Aitchison, 1986). To detect elemental associations with similar relative variation patterns that may be interpreted from a paleoenvironmental standpoint (e.g., von Eynatten et al., 2003, 2016; Montero-Serrano et al., 2010), a principal component (PCA) and a clustering analysis were performed on the major surface geochemical elements (Ti-Mn-Fe-Al-Si-K-Ca) from the XRF core scanner data set. Prior to multivariate analysis, a log-centered (clr) transform was applied (Aitchison, 1990). This transformation first divides the elemental concentration by the geometric mean of the composition of the individual observations and then, uses the logarithm. Note that all the geochemical element ratios are expressed in a log-ratio in order to minimize the highest values and distribute the lowest one, which is most suitable for right-skewed distributions (van den Boogaart and Tolosana-Delgado, 2013). PCA was conducted using the "CoDaPack" software (Thió-Henestrosa and Comas, 2011) and clustering analysis by using the Ward's method in "PAST" software. Finally, physical and magnetic properties, grain size and carbon-nitrogen data, as well as the score from the first principal component of the log-centered XRF data were used to produce interpolated maps using Ocean Data View (ODV) software (Schlitzer, 2018). The interpolated maps were generated using a weighted-average gridding algorithm with a quality limit of 1.5. Numerical data were summarized in Annexes 1, 2, 3.

4. Results

4.1. CHRONOLOGY

The chronology of seven box cores from the entire area (Fig. 1B) was established using the ^{210}Pb measurements. Clear radioactive decays are observed and allow to visually determining the value of the supported ^{210}Pb and finally the excess ^{210}Pb (Fig. 5). Thus, the slope of the unsupported ^{210}Pb decay has been used to calculate the sedimentation rates (SR; Fig. 5) and finally the basal ages of each dated cores. Generally, the sedimentation rates vary between ~82.3 and 370 cm/ka with basal ages from ~1550 to 1820 AD, suggesting a possibility to reconstruct the conditions since the last ~ 600 years and especially during the LIA.

These new sedimentation rate estimations are similar and complement the different data already obtained in the Mackenzie Shelf/Slope (Richerol et al., 2008; Schell, 2008; Bringué and Rochon, 2012; Durantou et al., 2012), the Amundsen Gulf (Schell et al., 2008), the Coronation Gulf (Pieńkowski et al., 2011; 2017) and the Victoria and Barrow Straits (Vare et al., 2009; Ledu et al., 2010a; 2010b; Belt et al., 2010; Pieńkowski et al., 2013). Finally, the age of the LIA in the CAA was already referenced between ~1550-1850 AD in the Mackenzie Shelf/Slope (Loso et al., 2006; Bringué and Rochon, 2011), ~1680-1940 AD in the Coronation Gulf (Pieńkowski et al., 2011; 2017) and ~1500-1900 AD in the Victoria Strait (Belt et al., 2010).

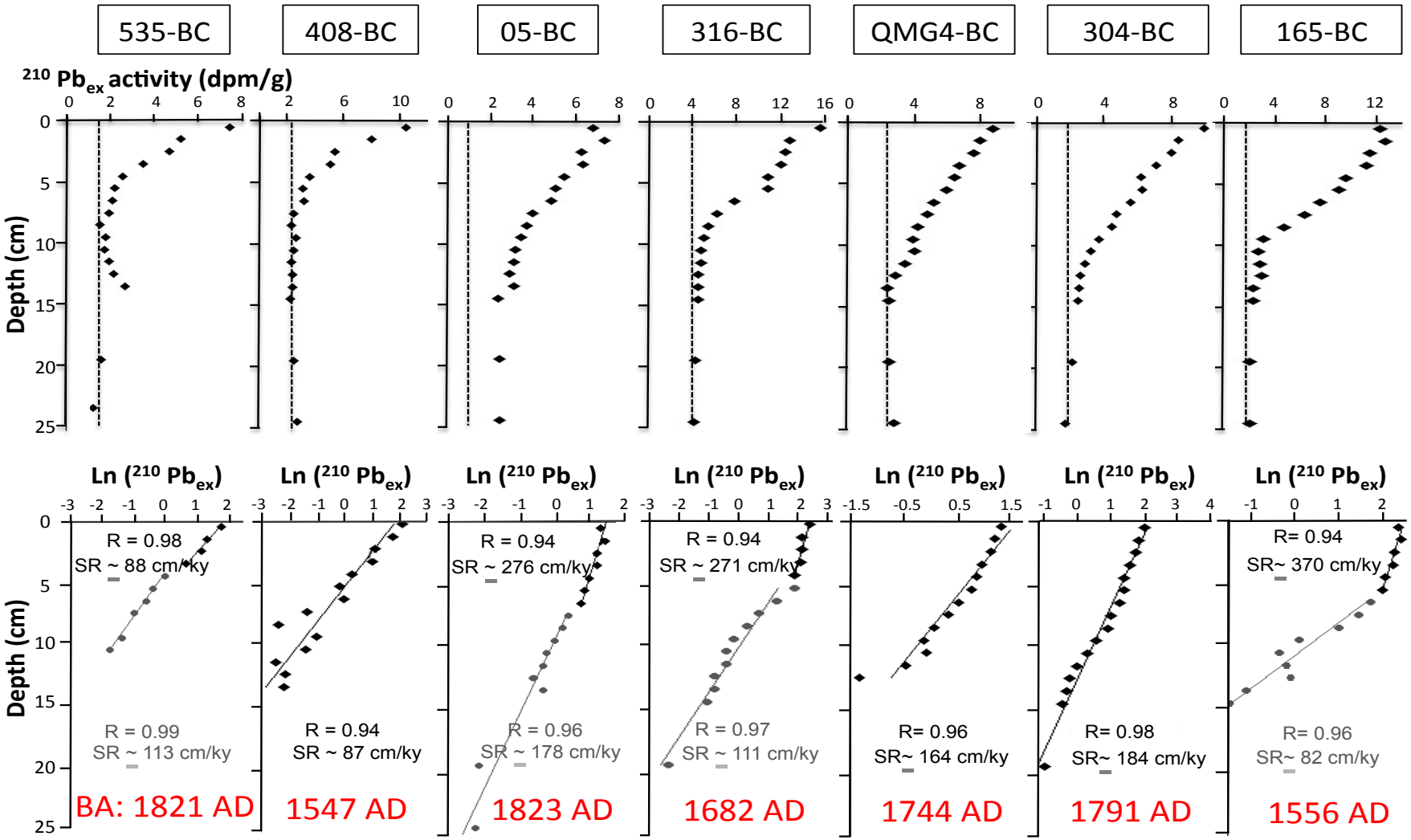
535-BC
408-BC
05-BC
316-BC
QMG4-BC
304-BC
165-BC
210 Pbex activity (dpm/g)
Depth (cm)
Ln (210 Pbex)
R = 0.98
SR ~ 88 cm/ky
R = 0.99
SR ~ 113 cm/ky
BA: 1821 AD
R = 0.94
SR ~ 87 cm/ky
1547 AD
R = 0.94
SR ~ 276 cm/ky
R = 0.96
SR ~ 178 cm/ky
1823 AD
R = 0.94
SR ~ 271 cm/ky
R = 0.97
SR ~ 111 cm/ky
1682 AD
R= 0.96
SR~ 164 cm/ky
1744 AD
R= 0.98
SR~ 184 cm/ky
1791 AD
R= 0.94
SR~ 370 cm/ky
R= 0.96
SR~ 82 cm/ky
1556 AD

Figure 5 ^{210}Pb chronology of selected bow cores from the CAA. Total activity of the ^{210}Pb (dpm/g) and vertical dashed lines characterized supported ^{210}Pb was represented in the first row. Ln (excess of ^{210}Pb activity) and basal age (BA) for each core were represented in the next ones.

4.2. SEDIMENTOLOGICAL AND PHYSICAL PROPERTIES

4.2.1. Grain size distribution

The mean surface and basal grain size in the study area do not depict great variability and are mainly composed of silts. Indeed, the mean surface sediment grain size (Fig. 6A) expressed in phi scale ranges from 9.0 (clay) to 7.0 (fine silt) where the minimum phi values are found in the Coronation Gulf. The surface samples grain size distribution shows a general West-East trend with finer grains (8-9 Φ) in the Western and coarser grains (< 8 Φ) in the Eastern part. The basal sample grain size shows a coarser grain size near to the Mackenzie mouth (~ 8.5 Φ), whereas the rest of the Western and Eastern parts generally become finer (7.5Φ).

Generally, sorting is better as the mean grain size decreases, especially in the West province surface sediments (Fig. 6B). The most poorly sorted sediments are found in the East and near to M'Clure Strait (545-BC and 20-BC). Moreover, surface sediments and basal East sediments are more widely dispersed suggesting spatial and temporal sedimentary processes variations.

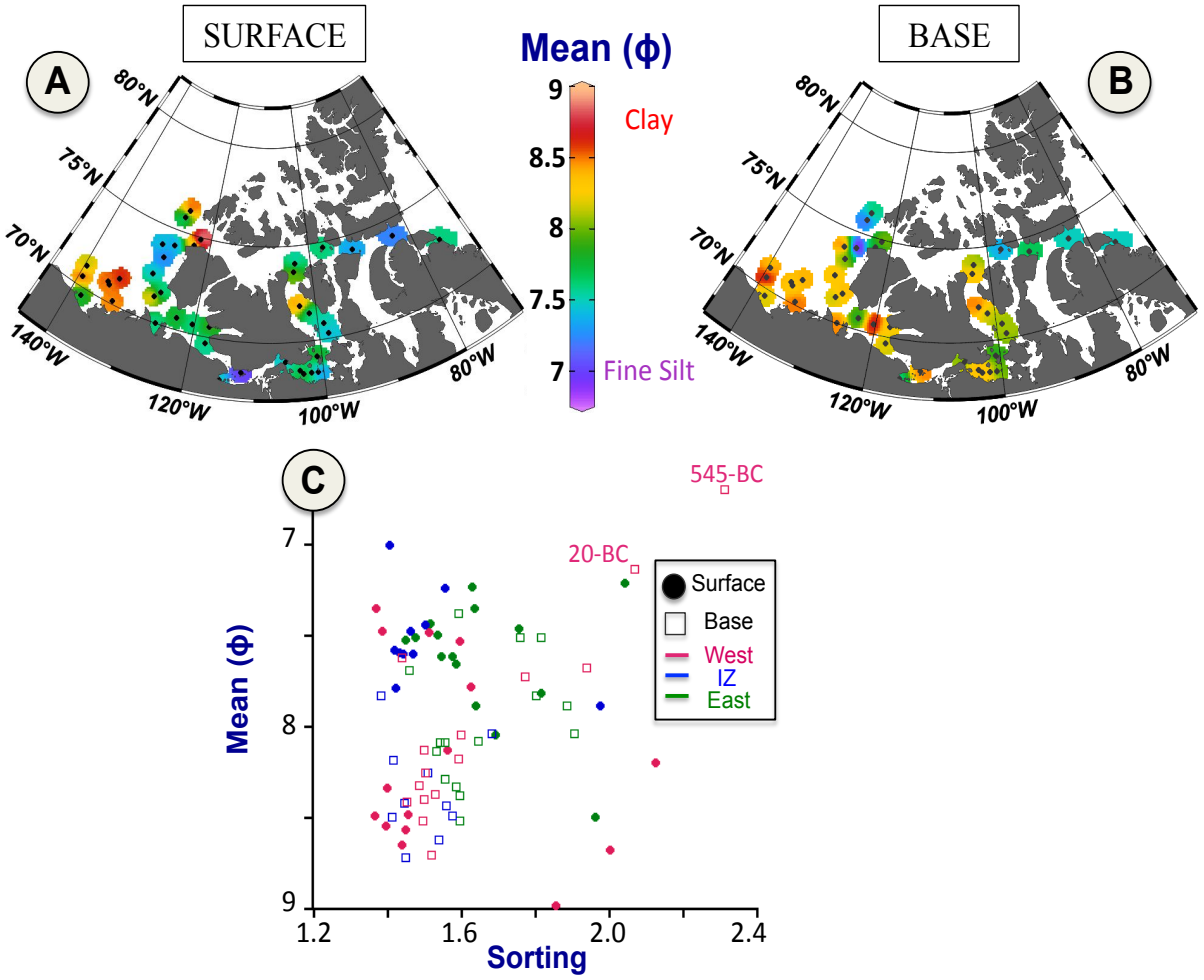

Figure 6 Maps of surface (A) and basal (B) mean grain size distributions. (C) Plot of sorting versus mean grain size in phi scale for surface and base sediment samples.

4.2.2. Spatial delimitations based on elemental geochemistry

Statistical analyses reveal three geographical clusters (Fig. 7A and 7B) with distinct geochemical compositions: the west (M'Clure strait, West Banks Island and the Mackenzie shelf/slope), the intermediate zone (the Amundsen, Coronation and Queen Maud Gulfs) and the east (Queen Maud Gulf, Victoria and Barrow Straits, Lancaster Sound). PCA for surface

(Fig. 7C) and basal (Fig. 7D) sediments reveal that the PC1-scores (representing 51.98 % of the total variance) are positively associated with detrital elements (Ti-Fe-Rb-Zn-Y) where most of the west stations are represented, whereas, the PC2-scores (19.17 % of total variance) are mostly associated to detrital carbonates (K-Ca) and east province stations. It is also important to mention that the Mn was removed from the PCA because of its large influence on geochemical variability.

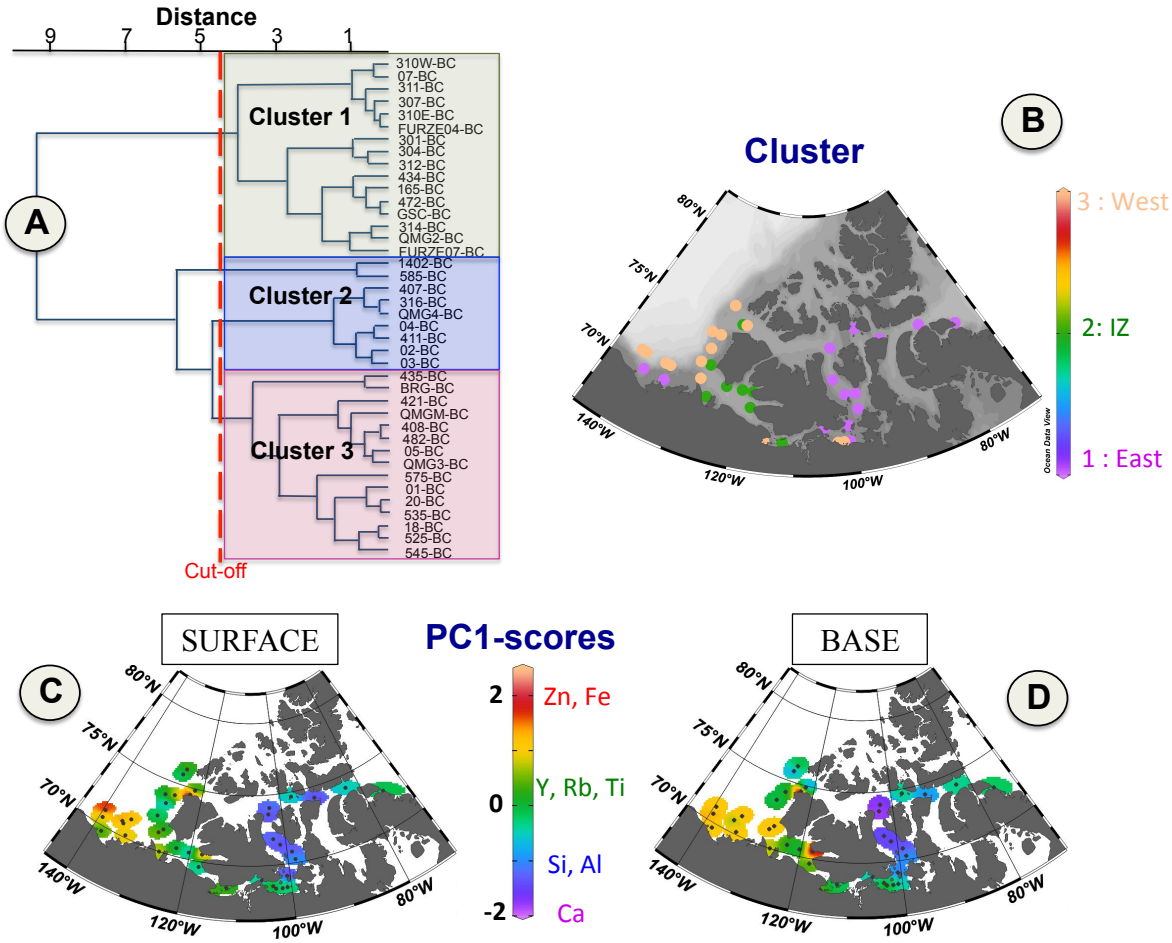

Figure 7 Statistical analysis based on major geochemical elements: (A) Clustering dendrogram; (B) map of the three clusters, which point out the three geographical provinces. PCA for surface (C) and basal (D) sediments revealing the main geochemical assemblages influence.

The Log(Mn/Al) distribution map show higher concentrations, for surface sediments (Fig. 7C) especially in the south of Banks Island, the Amundsen and Coronation Gulfs. Finally, Log(Al/Ca) is used as a sediment source and transport agent indicator. Indeed, higher Log(Al/Ca) values were found in the West Province for surface (Fig. 7E) and basal (Fig. 7F) sediments, whereas lower Log(Al/Ca) values were mostly observed in the East Province in the surface and basal sediments as well.

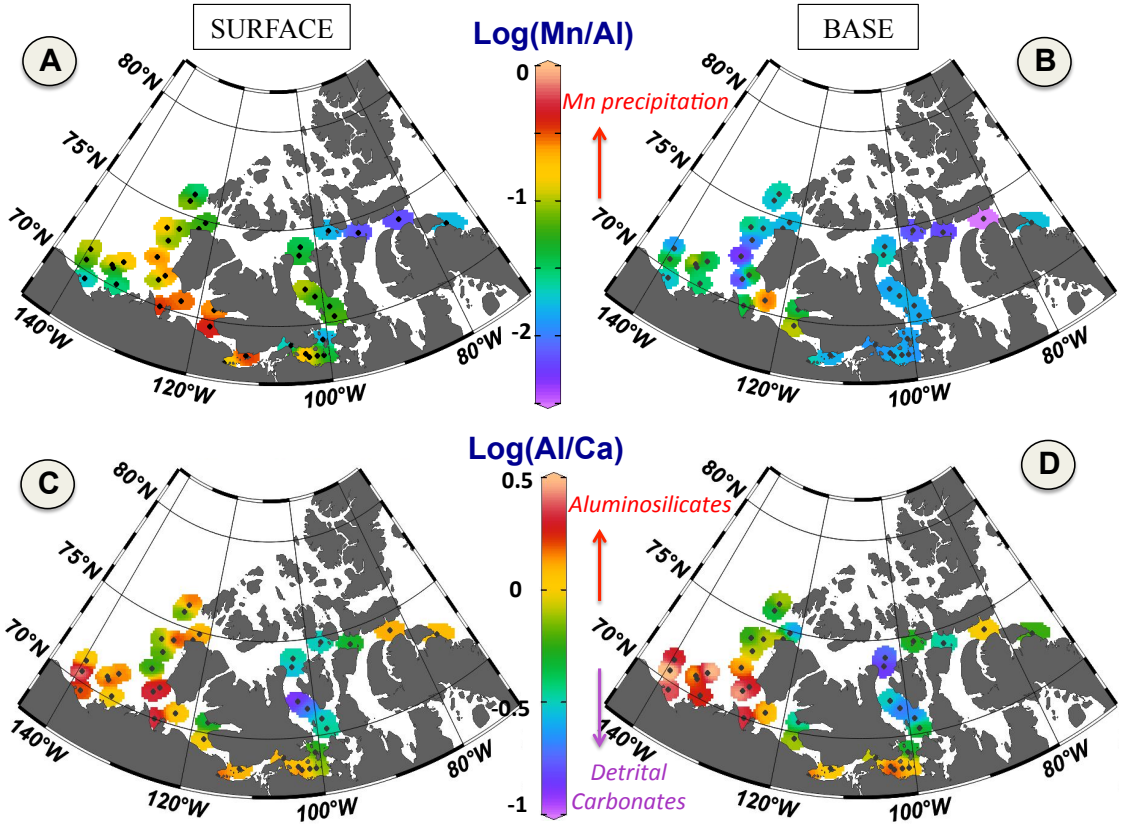

Figure 8 Log(Mn/Al) distribution for surface (A) and base (B) showing Mn precipitation in surface samples located in the south of Banks Island, the entrance of the Amundsen Gulf and part of the Coronation Gulf. Log(Al/Ca) using as sediment sources and transport indicators on the surface (C) and basal (D) samples.

4.2.3. Carbonate and inorganic carbon contents

Figure 9 illustrates the organic and inorganic carbon concentrations in the study area. In the surface samples, the organic carbon content distribution (Fig. 9A) shows higher concentrations in the West and along the Lancaster Sound. On the other hand, the East area is characterized by higher contents of inorganic carbon (Fig. 9C; 9D) for surface and basal sediments. Whereas the organic carbon (Fig. 9B) particularly decreases in the Mackenzie shelf/slope area.

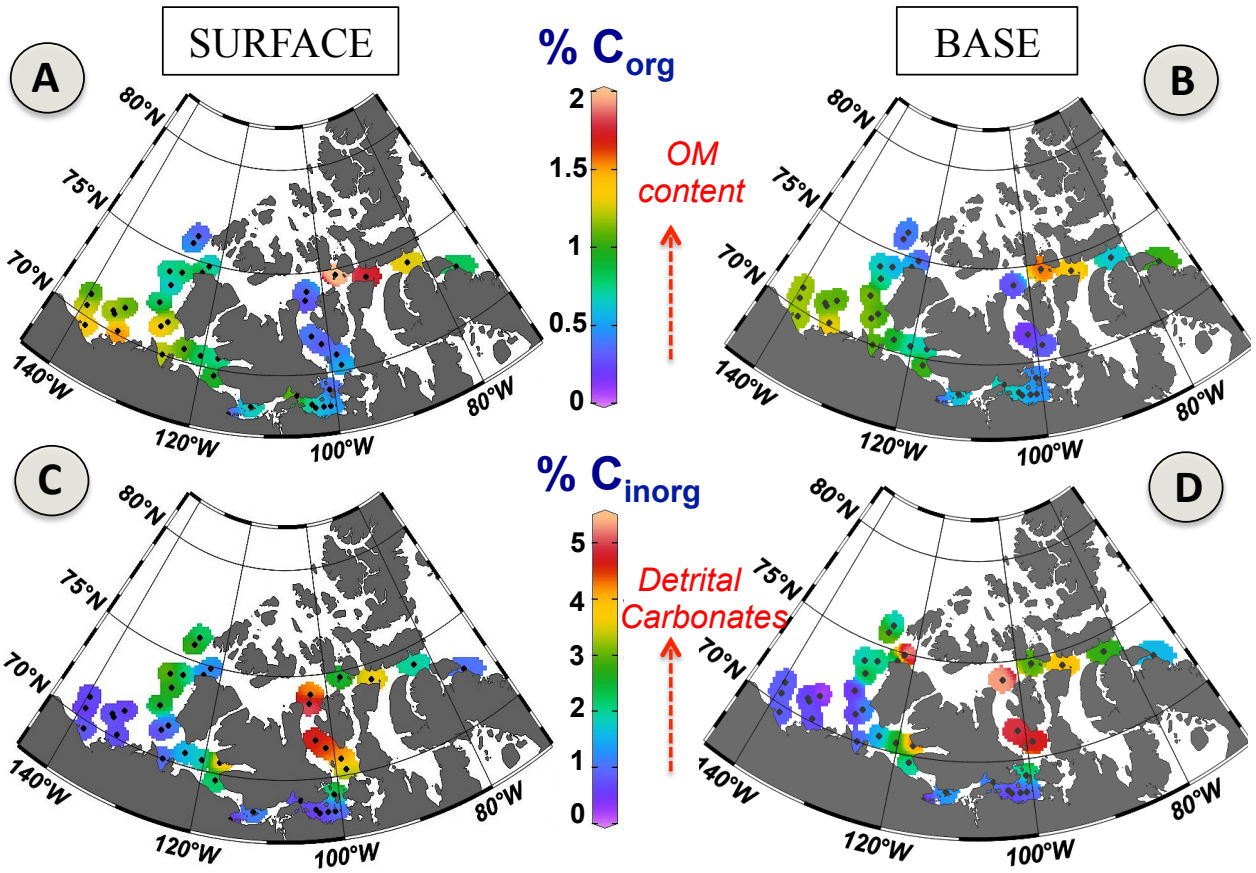

Figure 9 Maps of surface (A and C) and basal (B and D) organic carbon and inorganic carbon contents.

4.2.4. Organic carbon sources

Important information for paleoceanographic studies is to determine the origin of the organic matter (OM), to be then able to identify the sediment sources and finally reconstruct the sedimentary processes. To this end, we used the C/N ratio against $\delta^{13}C$ values as a mean to evaluate the OM sources (e.g., Meyers, 1994; St-Onge and Hillaire-Marcel, 2001; Fig. 10). The eastern province is firstly characterized by $\delta^{13}C$ values ranging from -22 to -23 ‰ in surface sediments, from -24 to -26 ‰ at the base and secondly by a C/N ratio between 5 to 10 in surface sediments and 5 to 15 in basal sediments. The western province is characterized by lower $\delta^{13}C$ values (from -24 to -26.5 ‰ in surface and from -26 to -30.5 ‰ at the base) and higher C/N values (from ~7 to 14 in surface sediments and from 5 to > 20 at the base). This plot consequently reveals a west-east trend with more terrigenous OM in the west, more marine OM in the east and a mixing between marine and terrigenous OM in the intermediate zone. Finally, the data also reveal that $\delta^{13}C$ values become lower whereas C/N ratio values are higher between the surface and the base of the sediment cores.

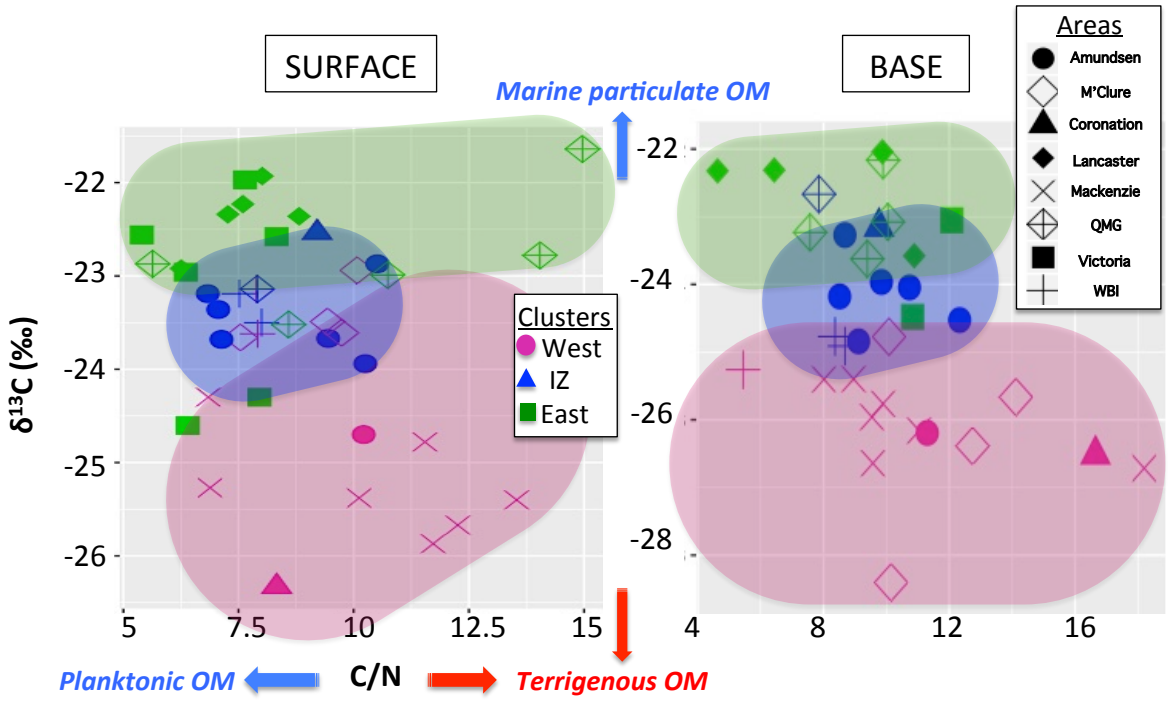

Figure 10 Relationship between C/N and $\delta^{13}C$ values. Three distinctive clusters of C/N and $\delta^{13}C$ values are highlighted and correspond to the three provinces previously identified. Amundsen = Amundsen Gulf; M'Clure= M'Clure Strait; Coronation= Coronation Gulf, Lancaster= Barrow Strait/Lancaster Sound; Mackenzie= Mackenzie Shelf/Slope; QMG= Queen Maud Gulf; Victoria= Victoria Strait and WBI= West Banks Island.

4.2.5. Sediment colours

The presence of detrital carbonates in the eastern part, more precisely in the Coronation Gulf and Victoria Strait; can also be determined with a whiter sediment colour expressed by higher L* values (Fig. 11A and 11B). L* values are relatively higher at the base than at the surface. Reddish sediments (Fig. 11C and 11D) are mainly observed in the Coronation and Queen Maud Gulfs both at the surface and base.

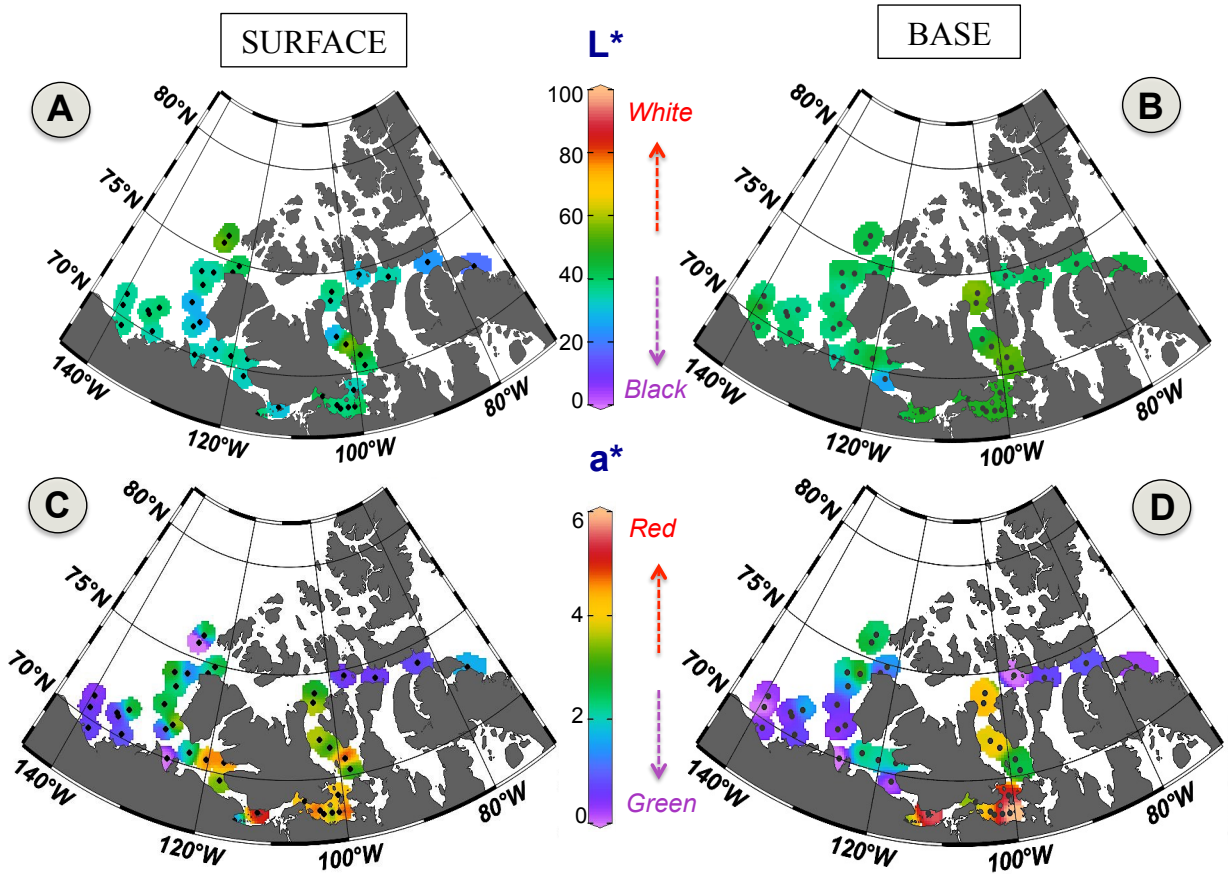

Figure 11 Spatial distributions of colour indices L* and a* for the surface and basal sediments.

4.3. MAGNETIC PROPERTIES

4.3.1. Frequency dependence

Difference in the magnetic susceptibility values between the low and high frequency is pretty negligible, suggesting the absence of superparamagnetic grains (Annexe. 4).

4.3.2. Magnetic mineralogy

The magnetic mineralogy in the CAA is mainly dominated by lower coercivity minerals such as magnetite. This is particularly supported by the pseudo S-ratio generally > 0.9, field saturation < 250 mT and the shapes of the hysteresis loops. In order to further discriminate sediment sources, we used the magnetic stability diagram of Maher and Thompson (1999) represented in Fig. 12A. This figure illustrates the "hardness" of the magnetic grains. Softer magnetic grains from the west to the east provinces and from surface to basal samples (except for the 05BC, Fig. 12B) are noticed. Moreover, the higher MDF_{NRM} values and wider hysteresis loop shapes (Fig. 12D) corresponding to the "harder" samples suggest a mixture of higher coercivity minerals with PSD/MD magnetite in the eastern part. In spite of this, the samples from the western part and the intermediate zone display softer coercivities with saturation fields < 100 mT and slender hysteresis loops shape (Fig. 12C) suggesting a dominance of low coercivity minerals such as magnetite.

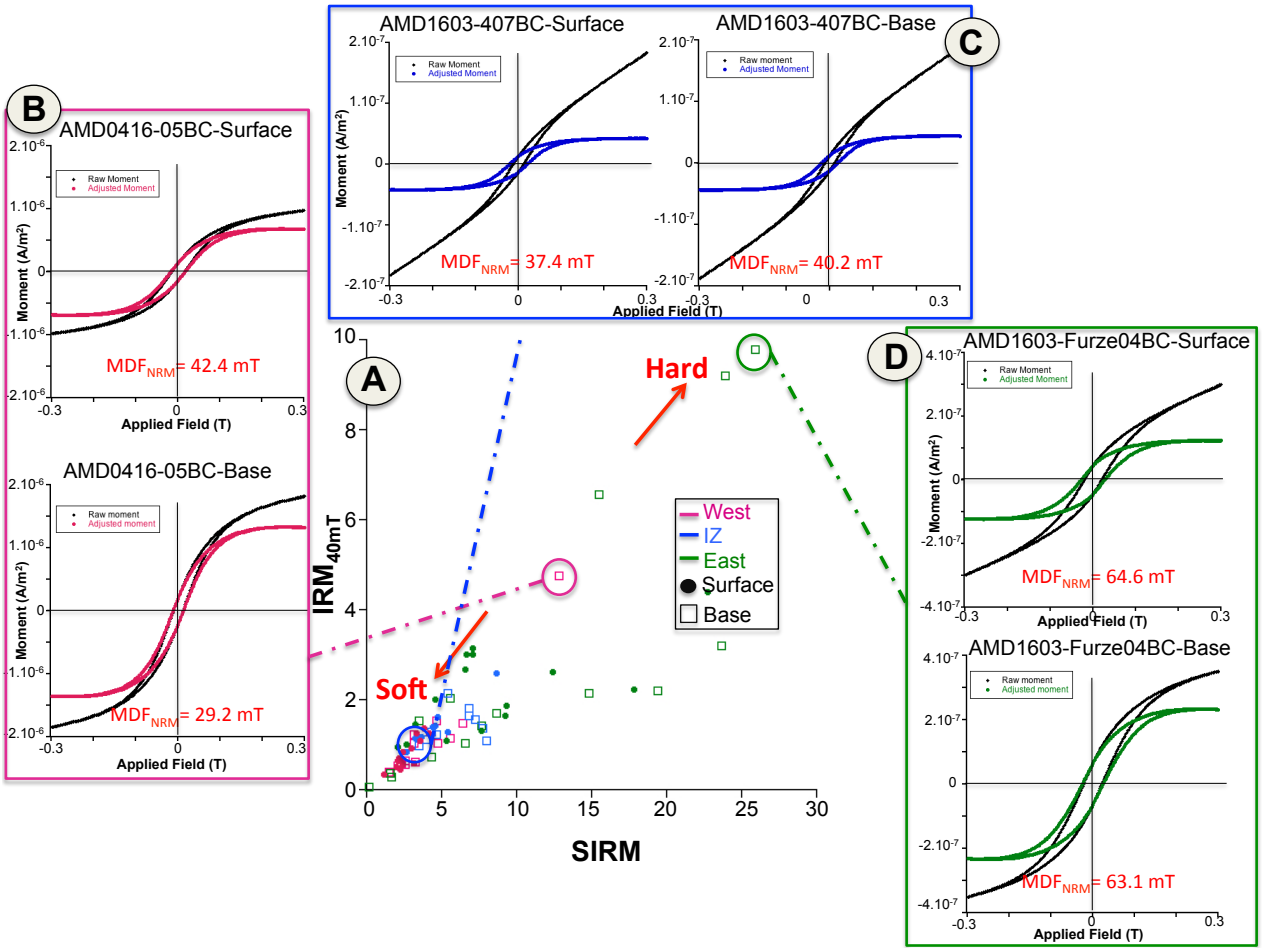

Figure 12 (A) Magnetic stability (Maher and Thompson, 1999). Hysteresis loops and MDF_{NRM} values for three representative cores: (B) 05BC (Coronation Gulf; West), (C) 407BC (Amundsen Gulf; IZ) and (D) Furze04-BC (Victoria Strait; East).

4.3.3. Magnetic concentration

In order to take a closer look at the magnetic grain concentration, a concentration-dependent parameter is used: magnetic susceptibility (k_{LF}; Fig. 13). Generally, the intermediate zone surface samples show high values of magnetic susceptiblity (k_{LF} > 25 x 10^{-5} SI) than anywhere else (k_{LF}=5 to 10 x 10^{-5} SI). This suggests a higher concentration of ferrimagnetic material in the intermediate zone whereas lower magnetic susceptibilities recorded in the western and

eastern areas could be due to the higher organic matter content in the west and higher detrital carbonate concentration in the east. Finally, magnetic susceptibility is mainly lower in the base compared to the surface sediment samples.

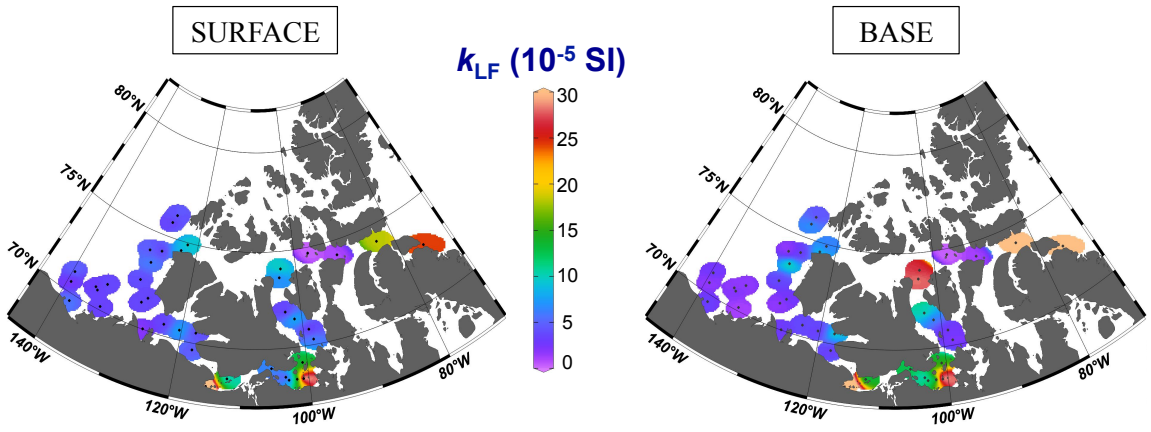

Figure 13 Spatial distribution of magnetic susceptibility (k_{LF}) for the surface and the basal sediments.

4.3.4. Magnetic grain size

The "Day plot" is useful to estimate the domain states of the magnetic grains and consequently, the magnetic grain size (Day et al., 1977; Dunlop, 2002*;* Fig. 14). A coarsening magnetic grain size trend is mainly observed between the surface and basal sediments, but also from west to east. Most samples are included in the pseudo-single domain (PSD) range and seem to be aligned to the theoretical single and multi-domain (SD + MD) mixing line. A larger contribution of coarser MD magnetite grains and other minerals is underlined for the east basal sediments and one west basal sample (AMD 2016-805-20BC). Otherwise, the rest of the samples are dominated by finer PSD magnetite grains.

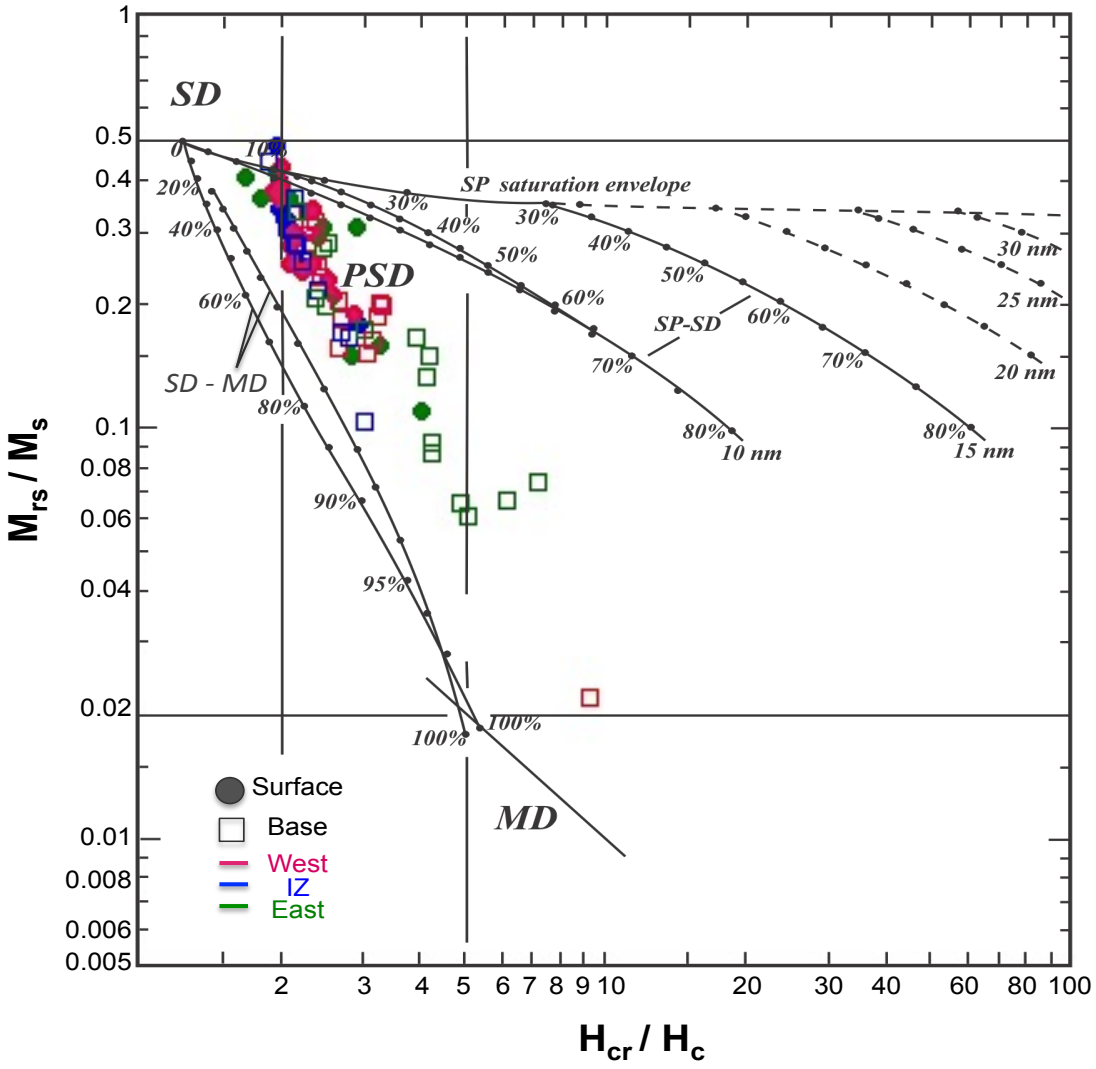

Figure 14 Day plot (Day et al., 1977) for the surface and basal samples. The mixing reference lines for single and multi-domain (SD and MD) are from Dunlop (2002).

4.4. RELATIONSHIP BETWEEN MAGNETIC PROPERTIES, GRAIN SIZE AND ELEMENTAL GEOCHEMISTRY

The relationship between the different properties was established by using bivariate graphs (Fig. 15). Firstly, the relation among mean-phi grain size and skewness (Fig. 15A) displays that surface sediments from East and IZ Provinces are mostly characterized by coarse detrital grain size and asymmetric samples. In return, surface sediments from the West Province and the majority of base sediment samples show the opposite trend. Given that, strongly skewed sediment samples with wide mean grain size variations are usually associated to environmental mixing zones such as river supply, sea ice and current transport. These observations therefore indicate relative contributions of different sediment processes acting within each province of the surface and the base. In addition, the relationship between the magnetic grain size (M_{rs}/M_s) and elemental geochemistry ratio (Fig. 15B) reveals a west-east trend where surface samples from the East Province is most characterized by fine magnetic grains (high M_{rs}/M_s ratio) and high content of detrital carbonates (low Al/Ca ratio) whereas West and IZ Provinces are influenced by high alluminosillicates concentrations.

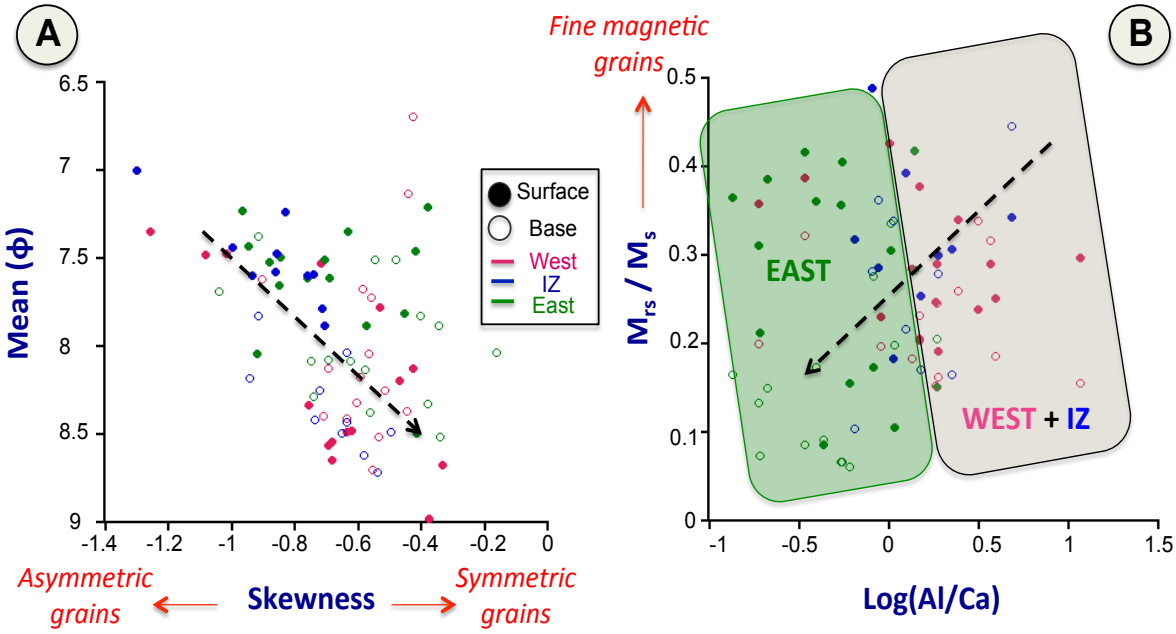

Figure 15 Relationships between mean detrital grain size in phi scale, skewness, magnetic grain size (M_{rs}/M_s) and elemental geochemistry [log(Al/Ca)].

5. Discussion

5.1. Sedimentary provinces and processes

As a result of the sedimentological, magnetic properties and the colour of the surface and basal sediments, three main provinces and their distinct sedimentary compositions and dynamic are described below and summarized in the Figs. 16 and 17.

5.1.1. The West Province

The surface sediments of the West (Mackenzie Shelf/Slope, West Banks Island and the M'Clure Strait) are mainly characterized by: fine detrital grains, detrital elements (Fe-Rb-Ti-Zn) associations and a dominance of aluminosilicates (high Al/Ca ratio), implying high detrital inputs delivered particularly by rivers. In this province, PSD magnetite and lower coercivity minerals (Figs. 12 and 14) were noticed, but even if magnetite is present, the magnetic susceptibility (k_{LF}; Fig. 13) remains relatively weak. This may be explained by the dilution of magnetic minerals by the large terrestrial OM supply (Fig. 10) coming from the Mackenzie River discharge (Macdonald et al., 1998; Magen et al., 2010; Gamboa et al., 2017). The homogeneous sedimentary composition within the Mackenzie Shelf/Slope, the relative symmetric grains and constant mean grain size (Fig. 15A) suggest a limited number of depositional processes. Modern sedimentation is, thus mainly dominated by the Mackenzie River discharge and supports the notion that the role of the Beaufort Sea, the Alaskan rivers or the coastal erosion in the Mackenzie Shelf/Slope is relatively insignificant (Hill et al., 1991; Gamboa et al., 2017). Moreover, differences in the sedimentary records observed within this province suggest that the Mackenzie plume influence is not strong enough to be the only common factor controlling the recent sedimentary processes in the West Banks Island and M'Clure Strait areas. Indeed, besides the high content in organic carbon found in the West Banks Island, confirming the influence of Mackenzie discharge, poorly sorted fine silts and detrital carbonate contents are higher compared to the Mackenzie Shelf/Slope. This likely suggests a modern supply by coastal cliff erosion of Quaternary dolomite-rich tills, in agreement with other studies in this area (O'Brien et al., 2006; Belliveau, 2007; Gamboa et al., 2017). Finally, in the M'Clure Strait region, the high contents of carbonate, phyllosilicates and the mixture of terrestrial and marine OM observed in surface sediments suggest a local sedimentation more influenced by the relatively constant 7-8m thickness sea-ice cover (McLaren et al., 1984; Canadian Ice Service- Environment Canada). Indeed, we assume that carbonates come from Banks Island (Darby et al., 2003) coastal erosion and bring into

M'Clure Strait by sea ice transport whereas phyllosilicates can probably come from the Mackenzie river discharge which was stucked inside the Beaufort Gyre before sea ice brings them in the M'Clure Strait.

The main sedimentary properties within the West Province remain substantially similar during the LIA (base samples): the geochemical element associations, the presence of SD/PSD magnetite and low coercivity minerals, along with a constant weak magnetic susceptibility associated with terrigenous organic matter inputs. Nevertheless, some differences can also be observed involving changes in the sedimentary processes. Detrital grain size becomes coarser near to the Mackenzie River mouth and finer around here, up to the north of Banks Island basal sediment samples (Fig, 6C) together with symmetric sediment samples. Moreover, the increase of aluminosilicate contents (higher Al/Ca ratio; Fig. 8D), until the north of Banks Island as well as the slight % C_{inorg} decrease (Fig. 9D) in the west of Banks Island could be explained by two possible scenarios. The first one suggests intensification and a wider influence of Mackenzie River supply between the beginning of the LIA (~1550 AD) and the current period. This is consistent with previous palynological studies (Richerol et al., 2008; Schell et al., 2008; Bringué and Rochon, 2012) along with McClelland et al (2006) who observed a ~ 4.5% decrease in annual discharge for the North American Arctic area between 1964 and 2000 AD. In contrast, a 2% increase of total annual discharge between 1964 and 2003 AD was identified (Déry and Wood, 2005; Déry et al., 2009; Shiklomanov and Shiklomanov, 2003) and a ~ 4-5% increase from the mid-Holocene to the preindustrial period (Wagner et al., 2011). On the other hand, increase of aluminosilicate contents directly brought by the river discharge suggests wetter and warmer conditions at the beginning of the LIA. Nevertheless, many of studies all around the area showed a cooling ~ 1550 AD (Loso et al., 2006; Anderson et al., 2007; Richerol et al., 2008; Bringué and Rochon, 2012). This leads us to our second scenario where the colder conditions during the LIA foster the cooling of the Beaufort Sea associated with the ice formation, promoting the entrainment of the sediment river supplied by the action of frazil ice and the suspension freezing sea ice transport (Reimnitz et al., 1990; 1992; Darby et al., 2003). This hypothesis is therefore supported by the

increase of asymmetric deposits and magnetic grain contents suggesting an implication of different deposit processes such as sea ice transport and river discharges and the work of oceanic currents.

Finally, since the sediments in the M'Clure Strait did not reach the LIA (Fig. 5), we cannot reconstruct changes in the sedimentary regime during the LIA for this region.

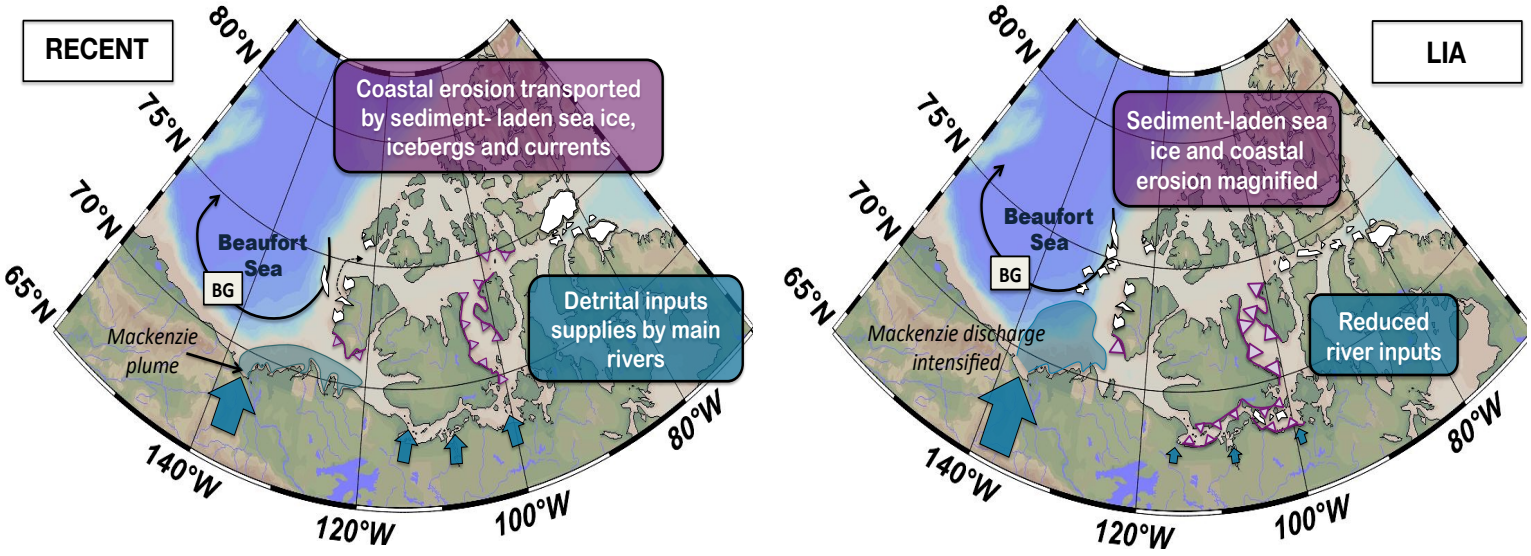

Figure 16 Sedimentary processes over the CAA during the LIA and the recent periods where blue arrows represent the river supplies and purple triangles characterize coastal erosion.

5.1.2: The Intermediate Province

The Intermediate Province (the Amundsen and Coronation Gulfs) acts as a transitional zone between the West and the East Provinces. The surface sediments are defined by common characteristics: Si-Al-Zr-Sr-K-Y contents, higher concentrations in manganese and aluminum (associated aluminosilicates), SD/PSD magnetite and a mixture of terrigenous and marine OM. The high concentrations in manganese observed in this region correlated with high values of a* (reddish sediment colour), indicating a geochemical relationship most likely similar to Fe-Mn oxyhydroxyde phases (Macdonald and Gobeil, 2012). In fact, a well-oxygenated water column sustained by a vertical turbulent mixing (strong winds and recurrent ice-free conditions) and high terrestrial OM input foster ideal conditions for the settling of Fe-Mn oxydroxyde onto the seafloor by reductive remobilization (Gamboa et al., 2017). Furthermore, some differences between the Amundsen and the Coronation Gulfs are also noteworthy. The high contents of poorly sorted clay-size sediments (~8 Φ), relatively high concentrations in terrestrial OM contents and low magnetic susceptibility found in the Amundsen Gulf reflect a modern sedimentation dominated by a strong influence of the far-reaching Mackenzie plume (Hill et al., 1991; Macdonald et al., 1998, Schell et al., 2008). In addition, the relative high content in detrital carbonates observed in the Amundsen Gulf demonstrates a further contribution of the coastal cliff erosion process (Belliveau, 2007) occurring in the south and west of Banks Island. The Coronation Gulf is in turn characterized by the predominance of detrital fine silts, asymmetric sediment samples, low concentrations in organic and inorganic carbon and a high magnetic susceptibility. These observations suggest that the local sedimentation is mainly influenced by surrounding rivers draining the Canadian Shield (e.g., Coppermine, Hayes and Ellice Rivers; Alkire et al., 2017). The predominance of riverine contributions in the local sedimentation suggest actual period of ice-free conditions and short sea ice conditions, which is consistent with previous studies (Turner et al., 2007; Pieńkowski et al., 2011; 2017).

The basal sediments describe some similarities with those from the surface: the elemental geochemistry is still dominated by the Si-Al-Sr-Zr-K-Y association, the detrital grain size is

generally finer, whereas the magnetic grain size is coarser along with the presence of low coercivity minerals such as magnetite. This may suggest that the sediment sources remained the same, and that some changes could be due to the contribution of different transport agents (such as sea ice transport; Pieńkowski et al., 2011; 2017). Additionally, a relatively high terrigenous OM content and the absence of the manganese precipitation (low Mn/Al ratio) suggest more anoxic conditions during the LIA compared to the most recent times, especially in the Coronation Gulf. In this latter area, the relatively higher magnetic susceptibility and concentration of reddish sediments in the LIA interval may indicate more continental inputs from the Canadian Shield during the LIA, supplied by coastal erosion and sea ice transport processes. This hypothesis is in agreement with the studies of Pieńkowski et al. (2011, 2017), that reconstructed colder conditions during the LIA with higher sea ice extent and a reduced open-water season.

5.1.3: The Eastern Province

Surface sediments of the Eastern Province indicate the main presence of fine silts (~7.5 Φ), a chemical composition generally dominated by calcium and marine OM. In addition, the magnetic properties reveal a weak magnetic susceptibility and a mixture of PSD low and high coercivity mineral mixture. However, specific differences within this province can also be observed. The Victoria and Barrow Straits show a large dominance of detrital carbonates supported by Log(Al/Ca) < -0.5 and C_{inorg} > 5%, suggesting that modern sedimentary processes are dominated by coastal erosion of Ordovician-Silurian carbonate-bearing rocks cropping out the Victoria and Prince of Wales Islands before they are ultimately transported by sediment-laden sea ice (Reimnitz et al., 1992; Darby et al., 2011). On the other hand, the high Log(Al/Ca) ratio in the Queen Maud Gulf indicates aluminosilicate enriched sediments (particularly feldspars; Belt et al., 2010; Deschamps et al., 2018). This suggests that sedimentary processes in this area are dominated by rivers discharge (e.g. Back, Hayes, Perry,

Armark and Simpson rivers), draining the Canadian Shield (Alkire et al., 2017). Moreover, the high content in phyllosilicates/aluminosillicates, terrigenous OM inputs and less from detrital carbonate inputs in the eastern Lancaster Sound can indicate sediments mainly transported by sea ice. The presence of glaciers on Devon Island and the Sirmilik National Park could have an impact on the settling by generating iceberg rafting and sediment-laden meltwater plumes sediment supply.

The base of the sediment cores in this Province is mainly characterized by relatively finer detrital grain size (~8.5 Φ), more poorly sorted, a dominance of the association of Ca-Si with a relatively weak magnetic susceptibility and more terrigenous sediment inputs compared to the surface. As opposed to the surface sediments, the magnetic mineralogy of the LIA sediments is dominated by higher coercivity minerals and a mixture of PSD/MD magnetite. Nevertheless, the relatively lower OM and higher detrital carbonate contents correlated with whiter sediments suggest that a more pronounced contribution of coastal erosion and sea ice sediment transport during the LIA compared with the present conditions. Actually, the clay sediments generally poorly sorted are commonly found in glaciated areas and deposited from sea ice. They are often associated to other material delivered from river supply, solufluction or mudflows from surrounding islands (Henderson, 1971). This observation suggests more intense ice conditions during the LIA, which was observed on the Devon Ice Cap and Ellesmere Island between 1550 and 1850 AD (Koerner and Paterson, 1974; Koerner et al., 1977; Koerner and Fisher, 1990; Bradley et al., 1990), Baffin Island (Penny Ice Cap) between 1400 and 1900 AD (Grumet et al., 2001), Victoria Strait between 1500 to 1900 AD (Belt et al., 2010; Peros and Gajewski, 2008; 2009), Boothia Peninsula (LeBlanc et al., 2004; Zabenskie and Gajewski, 2007), Prince Wales Island (Gajewski and Frappier, 2001), Somerset Island (Gajewski et al 1995) and Prescott Island (Finkelstein and Gajewski, 2007).

6. Conclusions

The regional sedimentary processes heterogeneity between recent and LIA conditions were investigated through magnetic, geochemical and sedimentological analyses of 40 surface and basal sediments throughout the CAA. The following conclusions are detailed below:

1. The multi-proxy analysis allowed the identification of three sedimentary provinces: (1) The West province (Mackenzie Shelf/Slope, the West of Banks Island and the M'Clure Strait) is typified by detrital associations (Fe-Rb-Ti-Zn), important organic matter inputs and higher Log(Al/Ca) ratio especially during the LIA; (2) The Intermediate Zone (Amundsen and Coronation Gulfs) is distinguished by Si-Al-Zr-Sr-K-Y associations, Fe-Mn oxyhydroxyde precipitation (particularly in the recent period), high magnetic susceptibility and a mixture between marine and terrigenous OM contents; (3) The Eastern province (Queen Maud Gulf, Victoria Strait and the Barrow/Lancaster Sound) is characterized by high detrital carbonate inputs, marine OM content, and low magnetic grain concentration.
2. The recent sedimentary processes are mainly influenced by the Mackenzie River discharge and its far-reaching plume in the Mackenzie Shelf/Slope and the Amundsen Gulfs, by little Canadian Arctic Archipelago rivers draining the Canadian Shield in the Coronation and Queen Maud Gulf whereas the Banks Island area, the M'Clure Strait and the East Province are mostly characterized by coastal erosion and sediment-laden sea ice.
3. The reconstructed LIA sedimentary processes suggest an intensification of the Mackenzie River runoff in the West and more intense sea ice conditions along with sediment laden sea ice and coastal erosion in the Intermediate zone and eastern Canadian Arctic Archipelago.
4. Our geochemical proxy Log(Al/Ca) ratio can be successfully used to track changes in the sedimentary sources within the Canadian Arctic Archipelago, where Al is associated to alluminosilicate discharged by rivers whereas Ca is coupled to detrital carbonates, coastal erosion and sea ice sediment-laden.

Globally, these new insights provide basis using sedimentological, geochemical and magnetic signatures from CAA sediments. And should be interesting for future studies that reconstruct variations in sediments settle and transport pathways related to Late Quaternary climate and oceanographic changes.

CONCLUSION GÉNÉRALE

Ce projet de maîtrise a employé une approche multi-traceurs : les propriétés sédimentologiques (granulométrie et origine de la matière organique), physiques (couleur des sédiments), géochimiques (éléments majeurs) et magnétiques (concentration, granulométrie et minéralogie magnétique). Ces analyses ont été faites à partir de carottes sédimentaires à boites échantillonnées à travers l'ensemble de l'Archipel arctique canadien. La comparaison spatiale des différentes propriétés a permis la séparation de cette zone d'étude en trois grandes provinces possédant chacune leur propre dynamique sédimentaire. Également, la comparaison temporelle des propriétés entre les échantillons de surface et de la base révèle une reconstruction des processus sédimentaires durant l'actuel et le Petit âge glaciaire (Fig. 17).

En effet, la sédimentation actuelle dans l'ouest est impactée par la décharge du Mackenzie, mais aussi par les apports détritiques provenant de l'érosion côtière de l'Île de Banks, transportant une partie des sédiments dans le détroit de M'Clure par la glace. Dans la zone intermédiaire, les sédiments proviennent de l'influence de la plume du Mackenzie, de l'érosion côtière de l'Île de Banks par la glace mais aussi des apports fluviatiles par les nombreuses petites rivières drainant le Bouclier canadien. Les processus sédimentaires actuels régissant l'Est sont moins homogènes : le golfe de la reine Maud est également influencé par les décharges fluviatiles de petites rivières tandis que les détroits de Victoria et de Barrow sont contrôlés par les apports détritiques de l'érosion côtière et du transport de sédiment par la glace. Dans le détroit de Lancaster, la présence actuelle de glaciers permet un apport de sédiment par les eaux de fonte saisonnières, formant des plumes de sédiments en suspension.

Durant le PAG, il a été montré une possible intensification de la décharge du Mackenzie à l'ouest en plus d'un transport de sédiment par *suspension freezing*. Les conditions sont plus froides et plus sèches dans la zone intermédiaire ainsi que dans la province de l'est. La glace joue donc un rôle plus important dans l'érosion des côtes et devient un agent de transport de sédiment

primordial dans ces deux provinces. De façon générale, les conclusions de cette étude rejoignent ceux précédemment publiées.

Finalement, ce projet de maîtrise montre bien l'utilité de coupler plusieurs traceurs qui décrivent des propriétés différentes mais aussi qui parfois se complémentent. Cette méthode peut être bénéfique notamment dans des zones d'étude aussi vastes, où les processus sédimentaires peuvent différer du tout au tout. De plus, il a été montré que le ratio géochimique Log(Al/Ca) peut être un très bon outil, en complément d'autres traceurs, permettant de retracer indirectement la variabilité des processus sédimentaires dans l'Archipel arctique canadien. Ce projet a également permis d'obtenir une vision spatiale des variations des processus sédimentaires avec comme points forts la datation de 7 carottes au ^{210}Pb, ce qui n'est pas toujours chose évidente dans l'Arctique.

Pour aller plus loin et dans l'intérêt de confirmer nos hypothèses quant à la dynamique sédimentaire durant le PAG, il serait intéressant d'utiliser la minéralogie mesurée au diffractomètre à rayons X (DRX). Ces données pourraient être ensuite comparées aux données de surface déjà obtenues dans la mer de Beaufort (Deschamps et al., 2018) ainsi que sur le plateau du Mackenzie et le golfe d'Amundsen (Gamboa et al., 2017). Étant donné que la signature minéralogique est déjà connue pour la province de l'ouest, ceci permettrait d'enrichir nos connaissances sur les changements de sources et de voies de transport entre la période actuelle et le PAG. Afin d'améliorer les qualités des données, les analyses minéralogiques (DRX) et géochimiques (XRF) pourraient être effectuées sur des pastilles qui limitent l'influence de l'humidité et de la taille granulométrique des grains. En outre, il serait essentiel de poursuivre les échantillonnages entrepris dans l'Archipel arctique canadien afin de continuer à combler les lacunes de cette mosaïque climatique qu'est l'Arctique. Ces nouvelles données pourraient être couplées à ces méthodes d'analyse mesurées en continu. Ceci permettrait d'obtenir une meilleure résolution ainsi que de nouvelles informations concernant les processus sédimentaires de la période du PAG, qui est finalement une période bien moins référencée dans l'Arctique que le dernier maximum glaciaire.

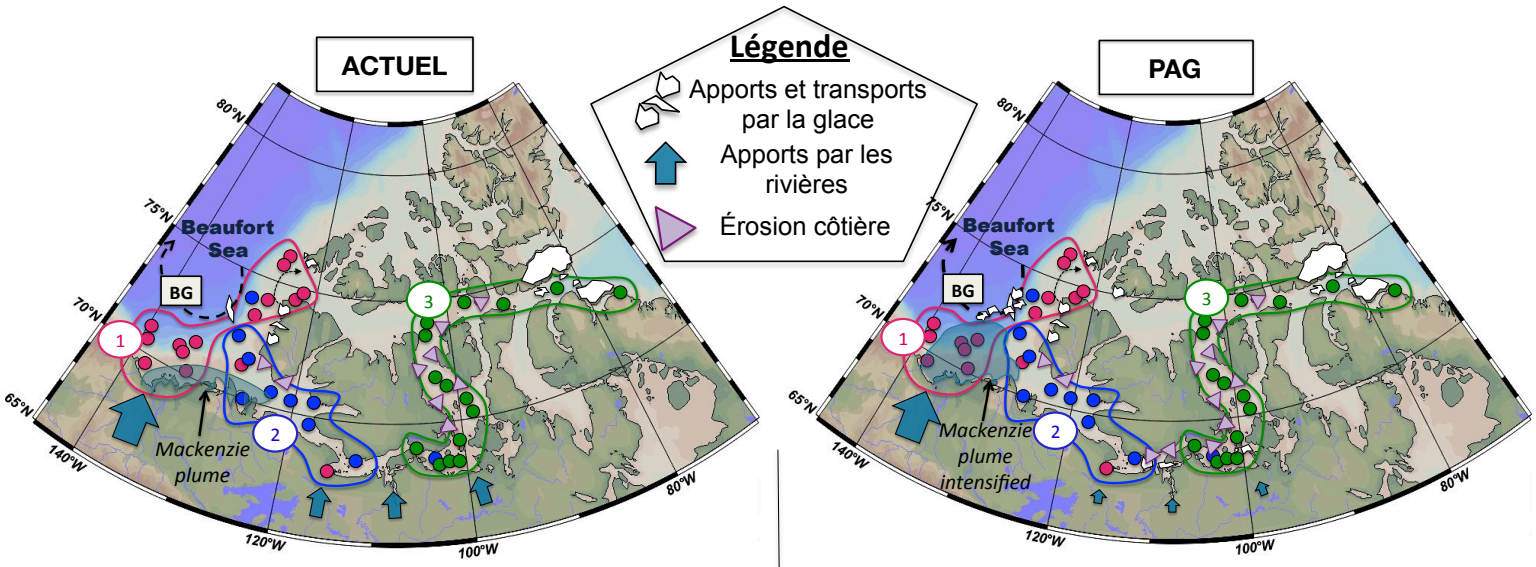

Forte influence de la décharge du Mackenzie + érosion côtière
Argiles, matière organique terrigène, aluminosilicates, faible k_{LF}, grains magnétique fins de faible coercivité

1

↑ **décharge du Mackenzie + influence mer de Beaufort**
Silts fins, matière organique terrigène, ↑aluminosilicates, faible k_{LF}, grains magnétique fins de faible coercivité

OUEST

Apports détritiques par les petites rivières du Bouclier canadien
Silts fins, sédiments rouges, matière organique terrigène et marine, haut k_{LF}, magnétite et minéraux de faible coercivité

2

Augmentation des conditions de glace + érosion côtière
Silts très fins, matière organique terrigène et marine, haut k_{LF}, magnétite et grains plus grossiers faible coercivité

ZI

Érosion côtière + transport par la glace
Silts fins, carbonates détritiques, matière organique marine, faible k_{LF}, minéraux grossiers de haute coercivité

3

Intensification de l'érosion côtière + transport par la glace
Silts très fins, ↑carbonates détritiques, matière organique marine, ↑ k_{LF}, minéraux grossiers de haute coercivité

EST

Figure 17 Résumé des propriétés caractérisant chaque province sédimentaire accompagné des processus sédimentaires mis en place durant le PAG et l'actuel.

ANNEXES

Annexe 1 : Sedimentological properties data from the studied cores.

	SURFACE							BASE						
Stations	**Mean (φ)**	**Sorting**	**Skewness**	**%Corg**	**%Cinorg**	**δ13C**	**C/N**	**Mean (φ)**	**Sorting**	**Skewness**	**%Corg**	**%Cinorg**	**δ13C**	**C/N**
01-BC	8,982	1,853	-0,376	0,620	1,240	-22,940	10,075	8,045	1,598	-0,569	0,090	5,390	-30,250	4,074
02-BC	7,788	1,421	-0,716	1,100	1,630	-23,670	9,448	7,830	1,379	-0,918	0,710	1,550	-26,120	9,620
03-BC	7,598	1,439	-0,935	0,770	1,740	-22,870	10,513	8,719	1,448	-0,541	0,500	2,720	-25,330	8,073
04-BC	7,575	1,418	-0,862	0,960	2,110	-23,360	7,062	8,178	1,413	-0,943	0,850	2,260	-25,400	10,773
05-BC	7,474	1,385	-1,018	0,330	0,560	-26,330	8,330	7,616	1,436	-0,905	0,180	0,630	-28,060	8,622
07-BC	8,493	1,960	-0,415	0,400	4,730	-22,580	8,326	8,514	1,594	-0,341	NA	NA	NA	NA
1402-BC	7,885	1,974	-0,706	0,720	4,010	-23,190	6,832	8,250	1,506	-0,724	0,440	4,600	-25,660	7,393
165-BC	7,610	1,573	-0,763	0,820	1,010	-22,360	8,815	7,504	1,758	-0,549	0,820	1,740	-23,960	12,794
18-BC	7,439	1,499	-1,001	0,740	3,070	-23,500	8,002	8,620	1,538	-0,582	0,430	1,790	-26,140	8,429
20-BC	7,531	1,592	-0,718	0,460	2,960	-23,660	7,543	7,132	2,066	-0,444	0,090	3,530	-29,090	4,060
301-BC	7,227	1,626	-0,967	1,290	1,960	-22,340	7,268	7,507	1,815	-0,481	0,410	2,960	-25,170	6,712
304-BC	7,351	1,632	-0,635	1,760	3,630	-22,230	7,595	7,687	1,456	-1,041	1,210	4,380	-23,760	10,923
307-BC	7,494	1,533	-0,847	0,370	4,150	-22,920	6,257	8,084	1,541	-0,625	0,090	5,330	-28,070	4,441
310E-BC	7,524	1,446	-0,883	0,390	4,240	-22,560	5,404	8,087	1,555	-0,749	0,090	4,390	-25,840	3,297
310W-BC	7,510	1,475	-0,706	0,300	4,450	-24,300	7,957	8,135	1,531	-0,580	NA	NA	NA	NA
311-BC	7,429	1,515	-0,948	0,580	3,360	-21,970	7,645	8,079	1,642	-0,696	0,020	3,580	-32,050	6,136
312-BC	7,815	1,813	-0,454	0,330	2,460	-22,960	6,354	7,827	1,799	-0,403	0,240	2,450	-25,730	9,946
314-BC	7,457	1,755	-0,421	1,100	0,720	-22,780	14,045	8,037	1,904	-0,165	0,440	1,300	-23,810	7,299
316-BC	6,998	1,402	-1,303	0,680	1,150	-24,680	8,931	8,488	1,572	-0,496	0,440	1,390	-24,870	9,698
407-BC	7,594	1,429	-0,742	1,220	0,980	-23,940	10,252	8,490	1,411	-0,653	0,820	0,910	-26,860	11,697
408-BC	8,331	1,398	-0,759	1,390	0,680	-24,700	10,218	8,125	1,497	-0,694	0,930	0,450	-27,510	13,383
411-BC	7,474	1,460	-0,858	1,200	1,200	-23,680	7,131	8,417	1,443	-0,739	0,770	1,370	-26,020	10,130
421-BC	8,647	1,436	-0,686	1,080	0,570	-24,300	6,845	8,413	1,451	-0,637	0,610	0,330	-26,120	6,831
434-BC	8,483	1,362	-0,638	1,540	0,700	-25,870	11,725	8,516	1,493	-0,537	0,950	0,650	-27,530	9,529
435-BC	8,122	1,561	-0,427	1,030	0,720	-25,380	10,117	8,366	1,526	-0,448	0,760	0,770	-28,760	9,975
472-BC	7,780	1,623	-0,534	1,370	0,850	-25,400	13,536	8,172	1,591	-0,595	0,880	0,800	-27,730	12,186
482-BC	8,564	1,448	-0,696	1,270	0,530	-24,780	11,547	8,699	1,518	-0,554	0,820	0,370	-27,330	9,064
525-BC	7,480	1,510	-1,085	0,790	2,620	-23,190	7,519	8,322	1,484	-0,607	0,560	2,690	-23,040	11,713
535-BC	7,233	1,554	-0,830	0,620	2,700	-23,140	7,889	8,038	1,680	-0,636	0,650	2,130	-26,190	20,936
545-BC	7,345	1,367	-1,261	0,790	2,060	-23,620	7,914	6,692	2,311	-0,429	0,310	2,180	-26,780	7,697
575-BC	8,672	2,000	-0,334	0,320	2,080	-23,490	9,432	7,675	1,936	-0,587	1,110	0,900	-21,460	48,427
585-BC	8,192	2,123	-0,469	0,950	1,180	-23,610	9,738	7,721	1,770	-0,558	0,630	1,220	-26,710	12,937
BRG-BC	8,540	1,392	-0,683	1,270	0,670	-25,270	6,883	8,395	1,496	-0,712	0,710	0,320	-27,510	9,202
FURZE04-BC	8,044	1,689	-0,921	0,260	5,140	-25,030	4,734	8,325	1,585	-0,380	NA	NA	NA	NA
FURZE07-BC	7,614	1,544	-0,690	2,030	2,490	-21,930	8,014	7,375	1,591	-0,918	1,480	2,670	-23,760	17,466
GSClander2-BC	8,482	1,452	-0,622	1,080	0,850	-25,670	12,260	8,252	1,501	-0,518	0,710	0,980	-27,800	23,662
QMG2-BC	7,209	2,041	-0,381	0,480	0,980	-22,870	5,637	7,881	1,884	-0,345	0,260	0,900	-24,280	7,026
QMG3-BC	7,881	1,638	-0,576	0,590	0,310	-24,230	6,771	8,288	1,554	-0,744	0,400	0,400	-25,990	7,912
QMG4-BC	7,595	1,467	-0,761	0,800	0,730	-23,140	7,908	8,431	1,558	-0,636	0,470	1,010	-24,880	9,022
QMGM-BC	7,655	1,582	-0,850	0,580	0,910	-23,520	8,589	8,378	1,593	-0,565	0,280	0,810	-24,790	64,469

Annexe 2: Physical and geochemical data from the studied cores.

	SURFACE				BASE			
Stations	**L***	**a***	**log (Al/Ca)**	**log (Mn/Al)**	**L***	**a***	**log (Al/Ca)**	**log (Mn/Al)**
01-BC	41,130	2,735	0,081	-1,282	42,410	1,610	-0,726	-1,746
02-BC	32,660	2,075	0,051	-0,533	39,680	2,410	0,167	-1,629
03-BC	37,620	4,740	-0,058	-0,716	45,940	2,100	-0,472	-1,781
04-BC	33,420	3,340	0,013	-0,374	24,830	0,020	0,493	-2,420
05-BC	39,670	1,540	0,181	-0,890	42,410	3,440	0,560	-1,475
07-BC	24,485	3,715	-0,905	-0,950	41,050	3,820	0,265	-1,519
1402-BC	35,220	4,675	0,500	-1,113	42,390	2,360	0,273	-1,961
165-BC	18,525	1,665	-0,021	-1,683	43,450	0,230	0,384	-1,728
18-BC	34,670	3,205	-0,171	-0,744	42,850	1,990	0,590	-1,241
20-BC	58,160	-2,300	-0,257	-0,984	43,140	2,810	0,129	NA
301-BC	24,500	0,755	0,118	-2,172	40,980	0,880	0,169	-2,042
304-BC	34,840	0,595	-0,305	-2,149	40,540	0,730	-0,049	-1,590
307-BC	39,715	2,745	-0,460	-1,457	58,340	4,290	1,065	-0,233
310E-BC	48,515	5,215	-0,488	-1,310	55,350	2,580	NA	NA
310W-BC	62,170	2,830	-0,685	-1,263	54,280	4,250	0,258	-1,965
311-BC	38,380	2,700	-0,462	-1,161	52,470	2,520	-0,470	-1,850
312-BC	32,510	4,270	-0,256	-1,889	48,630	5,230	-0,224	-1,734
314-BC	42,580	4,200	0,096	-1,753	47,160	3,360	0,007	NA
316-BC	30,690	5,160	0,100	-0,463	48,000	5,590	-0,413	NA
407-BC	34,250	-0,075	0,343	-0,447	35,070	-0,240	-0,726	-1,819
408-BC	34,180	0,210	0,347	-1,117	37,130	0,300	-0,678	-1,817
411-BC	25,450	4,240	0,301	-0,490	42,510	0,470	-0,724	-1,778
421-BC	39,460	3,150	0,157	-0,659	36,370	1,970	-0,271	-1,835
434-BC	34,130	0,855	-0,022	-1,562	39,550	0,710	-0,364	-1,856
435-BC	35,460	0,355	-0,041	-0,948	36,770	0,330	-0,087	-1,906
472-BC	36,555	0,685	0,205	-1,707	40,310	0,480	-0,874	-1,620
482-BC	35,870	0,550	0,483	-1,179	49,190	-0,240	-0,262	NA
525-BC	26,870	2,590	-0,119	-0,684	39,370	0,560	0,031	-2,003
535-BC	38,350	2,285	-0,201	-1,058	35,480	1,320	0,265	-1,713
545-BC	34,070	1,080	0,277	-1,091	42,370	3,580	0,142	-1,643
575-BC	47,240	3,500	0,241	-1,603	42,840	2,280	0,089	-0,537
585-BC	41,390	1,965	1,010	-1,405	38,770	0,370	-0,194	-1,217
BRG-BC	33,100	0,790	-0,033	-0,533	34,520	0,690	-0,098	-0,949
FURZE04-BC	34,415	3,755	-0,544	-1,329	54,300	4,340	0,679	-1,561
FURZE07-BC	30,440	0,495	-0,503	-1,766	38,390	-0,250	NA	NA
GSClander2-BC	44,350	0,160	0,320	-1,728	42,210	0,010	0,020	-1,813
QMG2-BC	44,790	5,655	-0,196	-1,553	47,470	6,790	0,344	-1,421
QMG3-BC	40,180	4,440	0,283	-0,959	47,630	4,610	0,270	-1,006
QMG4-BC	37,470	5,155	0,026	-0,353	47,870	3,940	-0,060	-2,025
QMGM-BC	34,200	1,830	0,008	-0,930	50,450	5,480	0,172	-1,940

Annexe 3: Magnetic properties from the studied cores.

	SURFACE						BASE					
Stations	**kLF**	**Mrs/Ms**	**Hcr/Hc**	**MDF(nrm)**	**IRM(40mt)**	**SIRM**	**kLF**	**Mrs/Ms**	**Hcr/Hc**	**MDF(nrm)**	**IRM(40mt)**	**SIRM**
01-BC	9,733	0,358	2,029	54,300	1,242	3,306	8,400	0,200	3,328	55,600	4,748	12,873
02-BC	3,383	0,395	2,006	69,800	1,163	3,701	6,400	0,282	2,180	40,300	1,280	4,348
03-BC	7,933	0,318	2,076	42,800	1,608	4,724	5,650	0,445	1,922	34,400	1,645	6,855
04-BC	4,800	0,489	1,993	45,300	1,386	4,400	5,830	0,253	2,282	41,700	1,216	4,682
05-BC	37,600	0,206	2,630	42,400	7,708	33,516	54,380	0,156	2,730	29,200	6,826	54,237
07-BC	2,967	0,418	1,991	71,600	2,994	6,677	11,650	0,284	2,574	67,800	6,556	15,496
1402-BC	4,050	0,343	2,030	46,800	1,412	4,618	10,970	0,218	2,463	39,200	1,806	6,851
165-BC	24,516	0,156	3,354	53,100	4,404	22,788	88,430	0,086	4,303	28,900	3,188	23,708
18-BC	4,883	0,321	2,100	48,200	1,153	3,247	3,120	0,338	2,194	49,600	2,144	5,432
20-BC	3,333	0,387	2,053	59,300	0,913	3,033	9,270	0,022	9,336	19,700	1,529	4,670
301-BC	18,367	0,305	2,974	47,000	2,610	12,389	42,250	0,061	5,137	21,500	2,151	14,814
304-BC	1,000	0,361	1,836	44,200	1,453	3,264	2,970	0,337	2,211	44,400	1,524	3,507
307-BC	10,400	0,311	2,507	68,500	2,665	6,598	22,330	0,174	3,098	63,500	9,204	23,886
310E-BC	2,933	0,387	0,505	38,200	2,014	4,555	4,900	0,134	4,177	17,400	0,279	1,631
310W-BC	8,600	0,212	0,337	67,900	3,139	7,066	8,380	0,150	4,227	11,400	2,021	5,607
311-BC	6,200	0,356	0,510	48,400	0,991	2,652	4,620	0,074	7,301	29,600	0,354	1,620
312-BC	13,514	0,086	0,216	42,100	1,312	7,690	13,480	0,067	6,200	31,100	1,030	6,550
314-BC	6,567	0,174	0,355	45,300	1,085	5,341	12,830	0,092	4,278	32,200	0,722	4,318
316-BC	9,970	0,183	3,021	15,000	2,571	8,707	12,480	0,165	2,861	30,200	1,364	7,738
407-BC	2,083	0,308	2,091	37,400	0,839	2,703	5,430	0,279	2,201	40,200	0,962	3,482
408-BC	3,883	0,240	2,261	48,400	0,628	2,113	3,550	0,205	2,700	35,000	0,567	2,564
411-BC	3,467	0,301	2,089	37,600	0,823	2,669	5,320	0,362	2,185	41,200	1,119	4,028
421-BC	3,933	0,291	2,228	8,300	0,687	2,173	3,880	0,323	2,372	36,600	1,219	3,156
434-BC	3,283	0,290	2,443	31,400	0,332	1,199	2,830	0,339	2,338	19,400	0,393	1,509
435-BC	5,150	0,192	2,928	35,300	0,551	2,393	5,320	0,317	2,413	38,100	0,557	2,376
472-BC	5,700	0,340	2,399	33,200	0,436	2,238	5,750	0,152	3,115	30,700	0,610	3,254
482-BC	2,167	0,251	2,383	34,900	0,669	2,289	3,600	0,247	2,434	34,700	0,589	2,301
525-BC	4,000	0,284	2,144	61,700	1,249	4,141	6,220	0,163	3,217	32,400	1,130	5,620
535-BC	6,150	0,286	2,183	35,400	1,397	4,398	11,880	0,171	2,746	21,600	1,091	7,966
545-BC	3,333	0,378	1,967	29,700	1,353	3,797	5,480	0,260	2,292	16,000	1,465	6,439
575-BC	4,600	0,231	2,594	34,700	0,842	2,436	6,600	0,186	3,281	32,000	1,018	3,192
585-BC	8,850	0,298	2,181	66,600	1,087	3,617	10,530	0,184	2,737	32,600	1,018	4,729
BRG-BC	2,567	0,427	2,043	33,900	0,503	1,966	3,630	0,232	2,482	34,100	0,633	2,550
FURZE04-BC	6,467	0,364	2,140	64,600	3,001	7,047	24,930	0,276	2,518	63,100	9,771	25,884
FURZE07-BC	0,333	0,407	1,717	55,500	0,940	2,073	0,800	0,165	3,960	49,000	0,056	0,142
GSClander2-BC	3,833	0,248	2,124	46,800	0,585	3,159	4,630	0,197	3,360	28,200	0,522	2,128
QMG2-BC	40,400	0,106	4,077	49,100	2,206	17,875	34,600	0,066	4,924	5,900	2,206	19,432
QMG3-BC	5,283	0,151	2,910	41,100	1,629	9,220	12,270	0,199	2,535	35,100	1,707	8,641
QMG4-BC	2,830	0,255	2,228	23,400	1,267	5,413	10,340	0,104	3,077	34,700	1,564	7,242
QMGM-BC	8,316	0,418	1,994	37,100	1,871	9,343	6,080	0,206	2,410	33,500	1,414	7,660

Annexe 4: Raw low frequency (k_{LF} 10^{-5} SI) and high frequency (k_{HF} 10^{-5} SI) susceptibilities.

	Surface		Base	
Stations	k_{LF}	k_{HF}	k_{LF}	k_{HF}
01BC	10	10	8	8
02BC	3	3	6	7
03BC	8	8	6	5
04BC	5	5	6	5
05BC	38	38	54	53
07BC	3	4	12	10
1402-BC	4	4	11	11
165BC	25	23	88	86
2016-805-18BC	5	5	3	3
2016-805-20BC	3	4	9	9
301BC	18	18	42	42
304BC	1	1	3	3
307BC	10	10	22	22
310E-BC	3	3	5	5
310W-BC	9	8	8	8
311BC	6	6	5	5
312BC	14	14	13	14
314BC	7	7	13	13
316-BC-A	10	9	12	12
407BC	2	2	5	5
408BC	4	4	3	3
411BC	3	4	5	5
421BC	4	4	4	4
434BC	3	1	3	3
435BC	5	5	5	6
472BC	6	6	6	5
482BC	2	3	4	3
525BC	4	4	6	6
535BC	6	6	12	11
545basic-BC	3	3	5	5
575BC	5	5	7	6
585BC	9	9	10	10
BRG-BC	3	3	4	4
Furze04-BC	6	6	25	24
Furze07-BC	0	1	1	1
GSCLander2-BC	4	4	5	5
QMG2-BC1	40	40	35	35
QMG3-BC	5	6	12	11
QMG4-BC	3	4	10	10
QMGM-BC	8	8	6	6

REFERENCES BIBLIOGRAPHIQUES

Aagaard, K., & Carmack, E. C. (1989). The role of sea ice and other fresh water in the Arctic circulation. *Journal of Geophysical Research: Oceans*, *94*(C10), 14485-14498.

Aagaard, K., & Carmack, E. 1. (1994). The Arctic Ocean and climate: A perspective. *The polar oceans and their role in shaping the global environment*, *85*, 5-20.

Aitchison, J. (1986). Monographs on Statistics and Applied Probability.

Aitchison, J. (1990). Relative variation diagrams for describing patterns of compositional variability. *Mathematical Geology*, *22*(4), 487-511.

Alkire, M. B., Jacobson, A. D., Lehn, G. O., Macdonald, R. W., & Rossi, M. W. (2017). On the geochemical heterogeneity of rivers draining into the straits and channels of the Canadian Arctic Archipelago. *Journal of Geophysical Research:* Biogeosciences, 122(10), 2527-2547.

Anderson, L., Abbott, M. B., Finney, B. P., & Burns, S. J. (2007). Late Holocene moisture balance variability in the southwest Yukon Territory, Canada. *Quaternary Science Reviews*, *26*(1-2), 130-141.

Andrews, J. T., & Eberl, D. D. (2012). Determination of sediment provenance by unmixing the mineralogy of source-area sediments: the "SedUnMix" program. *Marine Geology*, *291*, 24-33.

Appleby, P. G., & Oldfieldz, F. (1983). The assessment of 210Pb data from sites with varying sediment accumulation rates. *Hydrobiologia*, *103*(1), 29-35.

Aziz, O. I. A., & Burn, D. H. (2006). Trends and variability in the hydrological regime of the Mackenzie River Basin. *Journal of hydrology*, *319*(1-4), 282-294.

Barber, D. G., & Hanesiak, J. M. (2004). Meteorological forcing of sea ice concentrations in the southern Beaufort Sea over the period 1979 to 2000. *Journal of Geophysical Research: Oceans*, *109*(C6).

Beaudoin, J., & Hughes Clarke, J. (2004). A sound speed decision support system for multibeam sonar operations in the Canadian Arctic.

Belliveau, K. D. (2007). Coastal geomorphology of southwest Banks Island, NWT: historical and recent shoreline changes and implications for the future (Doctoral dissertation, Memorial University of Newfoundland).

Belt, S. T., Vare, L. L., Massé, G., Manners, H. R., Price, J. C., MacLachlan, S. E., ... & Schmidt, S. (2010). Striking similarities in temporal changes to spring sea ice occurrence across the central Canadian Arctic Archipelago over the last 7000 years. *Quaternary Science Reviews*, *29*(25-26), 3489-3504.

Bischof, J., Clark, D. L., & Vincent, J. S. (1996). Origin of ice‐rafted debris: Pleistocene paleoceanography in the western Arctic Ocean. *Paleoceanography*, *11*(6), 743-756.

Bischof, J. F., & Darby, D. A. (2000). Quaternary ice transport in the Canadian Arctic and extent of Late Wisconsinan Glaciation in the Queen Elizabeth Islands. *Canadian Journal of Earth Sciences*, *36*(12), 2007-2022.

Blott, S. J., & Pye, K. (2001). GRADISTAT: a grain size distribution and statistics package for the analysis of unconsolidated sediments. *Earth surface processes and Landforms*, *26*(11), 1237-1248.

Bradley, R. S. (1990). Holocene paleoclimatology of the Queen Elizabeth Islands, Canadian High Arctic. *Quaternary Science Reviews*, *9*(4), 365-384.

Bringué, M., & Rochon, A. (2012). Late Holocene paleoceanography and climate variability over the Mackenzie slope (Beaufort sea, Canadian Arctic). *Marine Geology*, *291*, 83-96.

Bintanja, R., & Selten, F. M. (2014). Future increases in Arctic precipitation linked to local evaporation and sea-ice retreat. *Nature*, *509*(7501), 479.

Burdige, D. J. (1993). The biogeochemistry of manganese and iron reduction in marine sediments. *Earth-Science Reviews*, *35*(3), 249-284.

Calvert, S. E., & Pedersen, T. F. (2007). Chapter fourteen elemental proxies for palaeoclimatic and palaeoceanographic variability in marine sediments: interpretation and application. *Developments in Marine Geology*, *1*, 567-644.

Carmack, E. C., & Macdonald, R. W. (2002). Oceanography of the Canadian Shelf of the Beaufort Sea: a setting for marine life. *Arctic*, 29-45.

Cohen, J., Screen, J. A., Furtado, J. C., Barlow, M., Whittleston, D., Coumou, D., ... & Jones, J. (2014). Recent Arctic amplification and extreme mid-latitude weather. *Nature geoscience*, *7*(9), 627.

Comiso, J. C., Parkinson, C. L., Gersten, R., & Stock, L. (2008). Accelerated decline in the Arctic sea ice cover. *Geophysical research letters*, *35*(1).

Comiso, J. C., Meier, W. N., & Gersten, R. (2017). Variability and trends in the A rctic S ea ice cover: Results from different techniques. *Journal of Geophysical Research: Oceans*, *122*(8), 6883-6900.

Croudace, I. W., Rindby, A., & Rothwell, R. G. (2006). ITRAX: description and evaluation of a new multi-function X-ray core scanner. *Geological Society, London, Special Publications*, *267*(1), 51-63.

Croudace, I. W., & Rothwell, R. G. (Eds.). (2015). Micro-XRF Studies of Sediment Cores: Applications of a non-destructive tool for the environmental sciences (Vol. 17). Springer.

Darby, D. A., Burckle, L. H., & Clark, D. L. (1974). Airborne dust on the Arctic pack ice, its composition and fallout rate. *Earth and Planetary Science Letters*, *24*(2), 166-172.

Darby, D. A., Bischof, J. F., & Jones, G. A. (1997). Radiocarbon chronology of depositional regimes in the western Arctic Ocean. *Deep Sea Research Part II: Topical Studies in Oceanography*, *44*(8), 1745-1757.

Darby, D. A. (2003). Sources of sediment found in sea ice from the western Arctic Ocean, new insights into processes of entrainment and drift patterns. Journal of Geophysical Research: Oceans, 108(C8).

Darby, D. A., Myers, W. B., Jakobsson, M., & Rigor, I. (2011). Modern dirty sea ice characteristics and sources: the role of anchor ice. *Journal of Geophysical Research: Oceans*, *116*(C9).

Day, R., Fuller, M., & Schmidt, V. A. (1977). Hysteresis properties of titanomagnetites: grain-size and compositional dependence. *Physics of the Earth and planetary interiors*, *13*(4), 260-267.

Dearing, J. (1999). Environmental magnetic susceptibility. *Using the Bartington MS2 system. Kenilworth, Chi Publ*.

Déry, S. J., & Wood, E. F. (2005). Decreasing river discharge in northern Canada. *Geophysical research letters*, *32*(10).

Déry, S. J., Hernández‐Henríquez, M. A., Burford, J. E., & Wood, E. F. (2009). Observational evidence of an intensifying hydrological cycle in northern Canada. *Geophysical Research Letters*, *36*(13).

Déry, S. J., Stadnyk, T. A., MacDonald, M. K., & Gauli-Sharma, B. (2016). Recent trends and variability in river discharge across northern Canada. *Hydrol. Earth Syst. Sci*, *20*(12), 4801-4818.

Deschamps, C. E., Montero‐Serrano, J. C., & St‐Onge, G. (2018). Sediment provenance changes in the western Arctic Ocean in response to ice‐rafting, sea‐level and oceanic circulation variations since the last deglaciation. *Geochemistry, Geophysics, Geosystems*.

Dickson, R., Rudels, B., Dye, S., Karcher, M., Meincke, J., & Yashayaev, I. (2007). Current estimates of freshwater flux through Arctic and subarctic seas. *Progress in Oceanography*, *73*(3-4), 210-230.

Dunlop, D. J. (2002). Theory and application of the Day plot (Mrs/Ms versus Hcr/Hc) 1. Theoretical curves and tests using titanomagnetite data. *Journal of Geophysical Research: Solid Earth*, *107*(B3), EPM-4.

Durantou, L., Rochon, A., Ledu, D., Massé, G., Schmidt, S., & Babin, M. (2012). Quantitative reconstruction of sea-surface conditions over the last~ 150 yr in the Beaufort Sea based on dinoflagellate cyst assemblages: the role of large-scale atmospheric circulation patterns. *Biogeosciences*, *9*(12).

England, J., Atkinson, N., Bednarski, J., Dyke, A. S., Hodgson, D. A., & Cofaigh, C. Ó. (2006). The Innuitian Ice Sheet: configuration, dynamics and chronology. *Quaternary Science Reviews*, *25*(7-8), 689-703.

Finkelstein, S. A., & Gajewski, K. (2007). A palaeolimnological record of diatom-community dynamics and late-Holocene climatic changes from Prescott Island, Nunavut, central Canadian Arctic. *The Holocene*, *17*(6), 803-812.

Forbes, D. L., & Taylor, R. B. (1994). Ice in the shore zone and the geomorphology of cold coasts. *Progress in Physical Geography*, *18*(1), 59-89.

Galley, R. J., Key, E., Barber, D. G., Hwang, B. J., & Ehn, J. K. (2008). Spatial and temporal variability of sea ice in the southern Beaufort Sea and Amundsen Gulf: 1980–2004. *Journal of Geophysical Research: Oceans*, *113*(C5).

Gajewski, K., Garneau, M., & Bourgeois, J. C. (1995). Paleoenvironments of the Canadian High Arctic derived from pollen and plant macrofossils: problems and potentials. *Quaternary Science Reviews*, *14*(6), 609-629.

Gajewski, K., & Frappier, M. (2001). A Holocene lacustrine record of environmental change in northeastern Prince of Wales Island, Nunavut, Canada. *Boreas*, *30*(4), 285-289.

Gajewski, K. (2002). Modern pollen assemblages in lake sediments from the Canadian Arctic. *Arctic, Antarctic, and Alpine Research*, *34*(1), 26-32.

Gajewski, K. (2006). Essai: Is Arctic Palynology a "Blunt Instrument"?. *Geographie physique et Quaternaire*, *60*(2), 95-102.

Gajewski, K. (2015). Quantitative reconstruction of Holocene temperatures across the Canadian Arctic and Greenland. *Global and Planetary Change*, *128*, 14-23.

Gamboa, A., Montero‐Serrano, J. C., St‐Onge, G., Rochon, A., & Desiage, P. A. (2017). Mineralogical, geochemical, and magnetic signatures of surface sediments from the Canadian Beaufort Shelf and Amundsen Gulf (Canadian Arctic). *Geochemistry, Geophysics, Geosystems*, *18*(2), 488-512.

Ghaleb, B. (2009). Overview of the methods for the measurement and interpretation of short-lived radioisotopes and their limits. In *IOP conference series: Earth and environmental science* (Vol. 5, No. 1, p. 012007). IOP Publishing.

Ghaleb, B., & Falguères, C. (2017). Apport des méthodes basées sur le déséquilibre radioactif (238U-234U-230Th-226Ra-210Pb) aux études des variations et changements climatiques. *L'Anthropologie*, *121*(1-2), 73-81.

Grumet, N. S., Wake, C. P., Mayewski, P. A., Zielinski, G. A., Whitlow, S. I., Koerner, R. M., ... & Woollett, J. M. (2001). Variability of sea-ice extent in Baffin Bay over the last millennium. *Climatic Change*, *49*(1-2), 129-145.

Harrison, J. C., Brent, T. A., & Oakey, G. N. (2011). Baffin Fan and its inverted rift system of Arctic eastern Canada: Stratigraphy, tectonics and petroleum resource potential. *Geological Society, London, Memoirs*, *35*(1), 595-626.

Helama, S., & Lindholm, M. (2003). Droughts and rainfall in south-eastern Finland since AD 874, inferred from Scots pine ring-widths. *Boreal Environment Research*, *8*(2), 171-183.

Henderson, P. J. (1971). Textural study of sediments of Barrow Strait, District of Franklin.

Hermanson, M. H. (1990). 210Pb and 137Cs chronology of sediments from small, shallow Arctic lakes. *Geochimica et Cosmochimica Acta*, *54*(5), 1443-1451.

Hill, P. R., Blasco, S. M., Harper, J. R., & Fissel, D. B. (1991). Sedimentation on the Canadian Beaufort Shelf. *Continental Shelf Research*, *11*(8-10), 821-842.

Hill, P. R., Lewis, C. P., Desmarais, S., Kauppaymuthoo, V., & Rais, H. (2001). The Mackenzie Delta: Sedimentary processes and facies of a high‐latitude, fine‐grained delta. *Sedimentology*, *48*(5), 1047-1078.

Holland, M. M., & Bitz, C. M. (2003). Polar amplification of climate change in coupled models. *Climate Dynamics*, *21*(3-4), 221-232.

Huntington, T. G. (2006). Evidence for intensification of the global water cycle: review and synthesis. *Journal of Hydrology*, *319*(1), 83-95.

Hyvärinen, H. (1985). Holocene pollen stratigraphy of Baird Inlet, east‐central Ellesmere Island, arctic Canada. *Boreas*, *14*(1), 19-32.

Ingram, R. G., & Prinsenberg, S. (1998). Coastal oceanography of Hudson Bay and surrounding eastern Canadian Arctic waters. *The sea*, *11*(29), 835-859.

Island, A. H., Island, V., Island, E., Territories, N., & Iqaluit, N. (2014). Canadian Arctic Archipelago. *Antarctica and the Arctic Circle: A Geographic Encyclopedia of the Earth's Polar Regions [2 volumes]*, 163.

Jakobsson, M. (2002). Hypsometry and volume of the Arctic Ocean and its constituent seas. *Geochemistry, Geophysics, Geosystems*, *3*(5), 1-18.

Jones, E. P., Swift, J. H., Anderson, L. G., Lipizer, M., Civitarese, G., Falkner, K. K., ... & McLaughlin, F. (2003). Tracing Pacific water in the North Atlantic ocean. *Journal of Geophysical Research: Oceans*, *108*(C4).

Kaufman, D. S., Ager, T. A., Anderson, N. J., Anderson, P. M., Andrews, J. T., Bartlein, P. J., ... & Dyke, A. S. (2004). Holocene thermal maximum in the western Arctic (0–180 W). *Quaternary Science Reviews*, *23*(5-6), 2529-2560.

King, J., Banerjee, S. K., Marvin, J., & Özdemir, Ö. (1982). A comparison of different magnetic methods for determining the relative grain size of magnetite in natural materials: some results from lake sediments. *Earth and Planetary Science Letters*, *59*(2), 404-419.

Koerner, R. M., & Paterson, W. S. B. (1974). Analysis of a core through the Meighen Ice Cap, Arctic Canada, and its paleoclimatic implications. *Quaternary Research*, *4*(3), 253-263.

Koerner, R. M. (1977). Devon Island ice cap: core stratigraphy and paleoclimate. *Science*, *196*(4285), 15-18.

Koerner, R. M., & Fisher, D. A. (1990). A record of Holocene summer climate from a Canadian high-Arctic ice core. *Nature*, *343*(6259), 630.

Kopec, B. G., Feng, X., Michel, F. A., & Posmentier, E. S. (2016). Influence of sea ice on Arctic precipitation. *Proceedings of the National Academy of Sciences*, *113*(1), 46-51.

Lammers, R. B., Shiklomanov, A. I., Vörösmarty, C. J., Fekete, B. M., & Peterson, B. J. (2001). Assessment of contemporary Arctic river runoff based on observational discharge records. *Journal of Geophysical Research: Atmospheres*, *106*(D4), 3321-3334.

LeBlanc, M., Gajewski, K., & Hamilton, P. B. (2004). A diatom-based Holocene palaeoenvironmental record from a mid-arctic lake on Boothia Peninsula, Nunavut, Canada. *The Holocene*, *14*(3), 417-425.

Ledu, D., Rochon, A., de Vernal, A., & St-Onge, G. (2008). Palynological evidence of Holocene climate change in the eastern Arctic: a possible shift in the Arctic oscillation at the millennial time scale. *Canadian Journal of Earth Sciences*, *45*(11), 1363-1375.

Ledu, D., Rochon, A., de Vernal, A., Barletta, F., & St‐Onge, G. (2010). Holocene sea ice history and climate variability along the main axis of the Northwest Passage, Canadian Arctic. *Paleoceanography and Paleoclimatology*, *25*(2).

Ledu, David, André Rochon, Anne de Vernal, and Guillaume St-Onge. "Holocene paleoceanography of the northwest passage, Canadian Arctic Archipelago." *Quaternary Science Reviews* 29, no. 25-26 (2010): 3468-3488.

Li, G., Piper, D. J., & Calvin Campbell, D. (2011). The Quaternary Lancaster Sound trough‐mouth fan, NW Baffin Bay. *Journal of Quaternary Science*, *26*(5), 511-522.

Linderholm, H. W., & Chen, D. (2005). Central Scandinavian winter precipitation variability during the past five centuries reconstructed from Pinus sylvestris tree rings. *Boreas*, *34*(1), 43-52.

Linderholm, H. W., Nicolle, M., Francus, P., Gajewski, K., Helama, S., Korhola, A., ... & Debret, M. (2018). Arctic hydroclimate variability during the last 2000 years. *Climate of the Past*.

Lisé-Pronovost, A., St-Onge, G., Gogorza, C., Haberzettl, T., Jouve, G., Francus, P., ... & Team, P. S. (2015). Rock-magnetic proxies of wind intensity and dust since 51,200 cal BP from lacustrine sediments of Laguna Potrok Aike, southeastern Patagonia. *Earth and Planetary Science Letters*, *411*, 72-86.

Ljungqvist, F. C., Krusic, P. J., Sundqvist, H. S., Zorita, E., Brattström, G., & Frank, D. (2016). Northern Hemisphere hydroclimate variability over the past twelve centuries. *Nature*, *532*(7597), 94.

Loso, M. G., Anderson, R. S., Anderson, S. P., & Reimer, P. J. (2006). A 1500-year record of temperature and glacial response inferred from varved Iceberg Lake, southcentral Alaska. *Quaternary Research*, *66*(1), 12-24.

Lotter, A. F., & Bigler, C. (2000). Do diatoms in the Swiss Alps reflect the length of ice-cover?. *Aquatic sciences*, *62*(2), 125-141.

Macdonald, R. W., Solomon, S. M., Cranston, R. E., Welch, H. E., Yunker, M. B., & Gobeil, C. (1998). A sediment and organic carbon budget for the Canadian Beaufort Shelf. *Marine Geology*, *144*(4), 255-273.

Macdonald, R. W., & Gobeil, C. (2012). Manganese sources and sinks in the Arctic Ocean with reference to periodic enrichments in basin sediments. *Aquatic Geochemistry*, *18*(6), 565-591.

MacLean, B., Williams, G. L., Srivastava, S. P., & Keen, M. J. (1990). Geology of Baffin Bay and Davis Strait. *Geology of Canada*, *2*, 293-348.

Magen, C., Chaillou, G., Crowe, S. A., Mucci, A., Sundby, B., Gao, A., ... & Sasaki, H. (2010). Origin and fate of particulate organic matter in the southern Beaufort Sea–Amundsen Gulf region, Canadian Arctic. *Estuarine, Coastal and Shelf Science*, *86*(1), 31-41.

Maher, B.A., & Thompson, R., eds. (1999). Quaternary climates, environments and magnetism . *Cambridge University Press*.

Manabe, S., & Stouffer, R. J. (1980). Sensitivity of a global climate model to an increase of CO2 concentration in the atmosphere. *Journal of Geophysical Research: Oceans*, *85*(C10), 5529-5554.

McClelland, J. W., Déry, S. J., Peterson, B. J., Holmes, R. M., & Wood, E. F. (2006). A pan‐arctic evaluation of changes in river discharge during the latter half of the 20th century. *Geophysical Research Letters*, *33*(6).

McLaren, A. S., Wadhams, P., & Weintraub, R. (1984). The sea ice topography of M'Clure Strait in winter and summer of 1960 from submarine profiles. *Arctic*, 110-120.

Melling, H., Gratton, Y., & Ingram, G. (2001). Ocean circulation within the North Water polynya of Baffin Bay. *Atmosphere-Ocean*, *39*(3), 301-325.

Melling, H. (2002). Sea ice of the northern Canadian Arctic Archipelago. *Journal of Geophysical Research: Oceans*, *107*(C11).

Meyers, P. A. (1994). Preservation of elemental and isotopic source identification of sedimentary organic matter. *Chemical geology*, *114*(3-4), 289-302.

Meyers, P. A. (1997). Organic geochemical proxies of paleoceanographic, paleolimnologic, and paleoclimatic processes. *Organic geochemistry*, *27*(5-6), 213-250.

Michel, C., Ingram, R. G., & Harris, L. R. (2006). Variability in oceanographic and ecological processes in the Canadian Arctic Archipelago. *Progress in Oceanography*, *71*(2-4), 379-401.

Millot, R., érôme Gaillardet, J., Dupré, B., & Allègre, C. J. (2003). Northern latitude chemical weathering rates: clues from the Mackenzie River Basin, Canada. *Geochimica et Cosmochimica Acta*, *67*(7), 1305-1329.

Montero-Serrano, J. C., Palarea-Albaladejo, J., Martín-Fernández, J. A., Martínez-Santana, M., & Gutiérrez-Martín, J. V. (2010). Sedimentary chemofacies characterization by means of multivariate analysis. *Sedimentary Geology*, *228*(3-4), 218-228.

Montero-Serrano, J. C., Rioux P., & Aebischer, S. (2016). Natural climate and oceanographic variability in the western Canadian Arctic Ocean since the last deglaciation. *ArcticNet Leg 3a Cruise Report - CCGS Amundsen (25 August to 17 September 2016)*.

Mosley‐Thompson, E., McConnell, J. R., Bales, R. C., Li, Z., Lin, P. N., Steffen, K., ... & Bathke, D. (2001). Local to regional‐scale variability of annual net accumulation on the Greenland ice sheet from PARCA cores. *Journal of Geophysical Research: Atmospheres*, *106*(D24), 33839-33851.

Mudie, P. J., & Rochon, A. (2001). Distribution of dinoflagellate cysts in the Canadian Arctic marine region. *Journal of Quaternary Science: Published for the Quaternary Research Association*, *16*(7), 603-620.

Nansen, F. (1902). The oceanography of the North Polar Basin. The Norwegian North Polar Expedition 1893-1896. *Scient. Results*, *3*(9).

Nichols, H. (1967). The disturbance of arctic lake sediments by "bottom ice": A hazard for palynology. *Arctic*, *20*, 213-214.

Nizou, J., Hanebuth, T. J., & Vogt, C. (2011). Deciphering signals of late Holocene fluvial and aeolian supply from a shelf sediment depocentre off Senegal (north‐west Africa). *Journal of Quaternary Science*, *26*(4), 411-421.

O'Brien, M. C., Macdonald, R. W., Melling, H., & Iseki, K. (2006). Particle fluxes and geochemistry on the Canadian Beaufort Shelf: implications for sediment transport and deposition. *Continental Shelf Research*, *26*(1), 41-81.

Oldfield, F., & Appleby, P. G. (1984). Empirical testing of 210 Pb-dating models for lake sediments. In *Lake sediments and environmental history*.

Overduin, P. P., Strzelecki, M. C., Grigoriev, M. N., Couture, N., Lantuit, H., St-Hilaire-Gravel, D., ... & Wetterich, S. (2014). Coastal changes in the Arctic. *Geological Society, London, Special Publications*, *388*, SP388-13.

Özdemir, Ö., & Dunlop, D. J. (1997). Effect of crystal defects and internal stress on the domain structure and magnetic properties of magnetite. *Journal of Geophysical Research: Solid Earth*, *102*(B9), 20211-20224.

Pachauri, R. K., Allen, M. R., Barros, V. R., Broome, J., Cramer, W., Christ, R., ... & Dubash, N. K. (2014). Climate change 2014: synthesis report. Contribution of Working Groups I, II and III to the fifth assessment report of the Intergovernmental Panel on Climate Change (p. 151). IPCC.

Paterson, W. S. B., & Waddington, E. D. (1984). Past Accumulation Rates at Camp Century and Devon Island, Deduced From Ice-Core Measurements. *Annals of Glaciology*, *5*, 222-223.

Peros, M. C., & Gajewski, K. (2008). Holocene climate and vegetation change on Victoria Island, western Canadian Arctic. *Quaternary Science Reviews*, *27*(3-4), 235-249.

Peros, M. C., & Gajewski, K. (2009). Pollen-based reconstructions of late Holocene climate from the central and western Canadian Arctic. *Journal of Paleolimnology*, *41*(1), 161-175.

Peterson, B. J., McClelland, J., Curry, R., Holmes, R. M., Walsh, J. E., & Aagaard, K. (2006). Trajectory shifts in the Arctic and subarctic freshwater cycle. *Science*, *313*(5790), 1061-1066.

Pieńkowski, A. J., Mudie, P. J., England, J. H., Smith, J. N., & Furze, M. F. (2011). Late Holocene environmental conditions in Coronation Gulf, southwestern Canadian Arctic Archipelago: evidence from dinoflagellate cysts, other non‐pollen palynomorphs, and pollen. *Journal of Quaternary Science*, *26*(8), 839-853.

Pieńkowski, A. J., England, J. H., Furze, M. F., Blasco, S., Mudie, P. J., & MacLean, B. (2013). 11,000 yrs of environmental change in the Northwest Passage: A multiproxy core record from central Parry Channel, Canadian High Arctic. *Marine Geology*, *341*, 68-85.

Pieńkowski, A. J., Gill, N. K., Furze, M. F., Mugo, S. M., Marret, F., & Perreaux, A. (2017). Arctic sea-ice proxies: Comparisons between biogeochemical and micropalaeontological reconstructions in a sediment archive from Arctic Canada. *The Holocene*, *27*(5), 665-682.

Pisaric, M. F., St-Onge, S. M., & Kokelj, S. V. (2009). Tree-ring reconstruction of early-growing season precipitation from Yellowknife, Northwest Territories, Canada. *Arctic, Antarctic, and Alpine Research*, *41*(4), 486-496.

Podritske, B., & Gajewski, K. (2007). Diatom community response to multiple scales of Holocene climate variability in a small lake on Victoria Island, NWT, Canada. *Quaternary Science Reviews*, *26*(25-28), 3179-3196.

Polyak, L., Curry, W. B., Darby, D. A., Bischof, J., & Cronin, T. M. (2004). Contrasting glacial/interglacial regimes in the western Arctic Ocean as exemplified by a sedimentary record from the Mendeleev Ridge. *Palaeogeography, Palaeoclimatology, Palaeoecology*, *203*(1-2), 73-93.

Porinchu, D. F., MacDonald, G. M., & Rolland, N. (2009). A 2000 year midge-based paleotemperature reconstruction from the Canadian Arctic archipelago. *Journal of Paleolimnology*, *41*(1), 177-188.

Prinsenberg, S. J., & Bennett, E. B. (1987). Mixing and transports in Barrow Strait, the central part of the Northwest Passage. *Continental Shelf Research*, *7*(8), 913-935.

Proshutinsky, A., Bourke, R. H., & McLaughlin, F. A. (2002). The role of the Beaufort Gyre in Arctic climate variability: Seasonal to decadal climate scales. *Geophysical Research Letters*, *29*(23), 15-1.

Rachold, V., Grigoriev, M. N., Are, F. E., Solomon, S., Reimnitz, E., Kassens, H., & Antonow, M. (2000). Coastal erosion vs riverine sediment discharge in the Arctic Shelf seas. *International Journal of Earth Sciences*, *89*(3), 450-460.

Reimnitz, E., & Maurer, D. K. (1979). Effects of storm surges on the Beaufort Sea coast, northern Alaska. *Arctic*, 329-344.

Reimnitz, E., & Barnes, P. W. (1987). Sea-ice influence on Arctic coastal retreat. In Coastal Sediments' 87, Proceedings of a Specialty Conference on Advances in Understanding of Coastal Sediment Processes. (Vol. 2, pp. 1578-1591).

Reimnitz, E., Barnes, P. W., & Harper, J. R. (1990). A review of beach nourishment from ice transport of shoreface materials, Beaufort Sea, Alaska. *Journal of Coastal Research*, 439-469.

Reimnitz, E., Clayton, J. R., Kempema, E. W., Payne, J. R., & Weber, W. S. (1993). Interaction of rising frazil with suspended particles: tank experiments with applications to nature. *Cold Regions Science and Technology*, *21*(2), 117-135.

Richerol, T., Rochon, A., Blasco, S., Scott, D. B., Schell, T. M., & Bennett, R. J. (2008). Evolution of paleo sea-surface conditions over the last 600 years in the Mackenzie Trough, Beaufort Sea (Canada). *Marine Micropaleontology*, *68*(1-2), 6-20.

Ruppel, M., Väliranta, M., Virtanen, T., & Korhola, A. (2013). Postglacial spatiotemporal peatland initiation and lateral expansion dynamics in North America and northern Europe. *The Holocene*, *23*(11), 1596-1606.

Schell, T. M., Moss, T. J., Scott, D. B., & Rochon, A. (2008). Paleo–sea ice conditions of the Amundsen Gulf, Canadian Arctic Archipelago: Implications from the foraminiferal record of the last 200 years. *Journal of Geophysical Research: Oceans*, *113*(C3).

Schlitzer, R. (2018). Ocean Data View, https://odv.awi.de.

Scott, D. B., Schell, T., St‐Onge, G., Rochon, A., & Blasco, S. (2009). Foraminiferal assemblage changes over the last 15,000 years on the Mackenzie‐Beaufort Sea Slope and Amundsen Gulf, Canada: Implications for past sea ice conditions. *Paleoceanography*, *24*(2).

Serreze, M. C., & Francis, J. A. (2006). The Arctic amplification debate. *Climatic change*, *76*(3-4), 241-264.

Serreze, M. C., Holland, M. M., & Stroeve, J. (2007). Perspectives on the Arctic's shrinking sea-ice cover. *science*, *315*(5818), 1533-1536.

Serreze, M. C., Barrett, A. P., Stroeve, J. C., Kindig, D. N., & Holland, M. M. (2008). The emergence of surface-based Arctic amplification. *The Cryosphere Discussions*, *2*(4), 601-622.

Serreze, M. C., & Stroeve, J. (2015). Arctic sea ice trends, variability and implications for seasonal ice forecasting. Phil.

Shaw, J., Taylor, R. B., Forbes, D. L., Ruz, M. H., & Solomon, S. (1998). *Sensitivity of the coasts of Canada to sea-level rise*(p. 114). Ottawa: Geological Survey of Canada.

Shiklomanov, I. A., & Shiklomanov, A. I. (2003). Climatic change and the dynamics of river runoff into the Arctic Ocean. *Water Resources*, *30*(6), 593-601.

Smol, J. P., Wolfe, A. P., Birks, H. J. B., Douglas, M. S., Jones, V. J., Korhola, A., ... & Brooks, S. J. (2005). Climate-driven regime shifts in the biological communities of arctic lakes. *Proceedings of the National Academy of Sciences*, *102*(12), 4397-4402.

St-Hilaire-Gravel, D., Bell, T. J., & Forbes, D. L. (2010). Raised gravel beaches as proxy indicators of past sea-ice and wave conditions, Lowther Island, Canadian Arctic Archipelago. *Arctic*, 213-226.

St-Hilaire-Gravel, D., Forbes, D. L., & Bell, T. (2011). Multitemporal analysis of a gravel-dominated coastline in the central Canadian Arctic Archipelago. *Journal of Coastal Research*, *28*(2), 421-441.

St-Hilaire-Gravel, D. (2012). *Arctic gravel beach morphodynamics under changing relative sea level and environmental forcing, Canadian Arctic Archipelago* (Doctoral dissertation, Memorial University of Newfoundland).

St-Onge, G., & Hillaire-Marcel, C. (2001). Isotopic constraints of sedimentary inputs and organic carbon burial rates in the Saguenay Fjord, Quebec. *Marine Geology*, *176*(1-4), 1-22.

St-Onge, G., Mulder, T., Francus, P., & Long, B. (2007). Chapter two continuous physical properties of cored marine sediments. *Developments in marine geology*, *1*, 63-98.

Stokes, C. R., Clark, C. D., Darby, D. A., & Hodgson, D. A. (2005). Late Pleistocene ice export events into the Arctic Ocean from the M'Clure Strait ice stream, Canadian Arctic Archipelago. *Global and Planetary Change*, *49*(3-4), 139-162.

Stokes, C. R., Clark, C. D., & Storrar, R. (2009). Major changes in ice stream dynamics during deglaciation of the north-western margin of the Laurentide Ice Sheet. *Quaternary Science Reviews*, *28*(7-8), 721-738.

Stoner, J. S., & St-Onge, G. (2007). Chapter three magnetic stratigraphy in paleoceanography: reversals, excursions, paleointensity, and secular variation. *Developments in Marine Geology*, *1*, 99-138.

Stroeve, J. C., Maslanik, J., Serreze, M. C., Rigor, I., Meier, W., & Fowler, C. (2011). Sea ice response to an extreme negative phase of the Arctic Oscillation during winter 2009/2010. *Geophysical Research Letters*, *38*(2).

Tauxe, L. (2010). *Essentials of paleomagnetism*. Univ of California Press.

Thio-Henestrosa, S., & Comas, M. (2011). CoDaPack v2 user's guide. Girona, Spain, University of Girona, Dept. of Computer Science and Applied Mathematics. from http://ima. udg. edu/codapack/assets/codapack-manual. pdf.

Turekian, K. K., Nozaki, Y., & Benninger, L. K. (1977). Geochemistry of atmospheric radon and radon products. *Annual Review of Earth and Planetary Sciences*, *5*(1), 227-255.

Turner, J., Overland, J. E., & Walsh, J. E. (2007). An Arctic and Antarctic perspective on recent climate change. *International Journal of Climatology*, *27*(3), 277-293.

Vare, L. L., Masse, G., Gregory, T. R., Smart, C. W., & Belt, S. T. (2009). Sea ice variations in the central Canadian Arctic Archipelago during the Holocene. *Quaternary Science Reviews*, *28*(13-14), 1354-1366.

Viau, A. E., & Gajewski, K. (2009). Reconstructing millennial-scale, regional paleoclimates of boreal Canada during the Holocene. *Journal of Climate*, *22*(2), 316-330.

Van den Boogaart, K. G., & Tolosana-Delgado, R. (2013). *Analyzing compositional data with R* (Vol. 122). Berlin: Springer.

von Eynatten, H., Barceló-Vidal, C., & Pawlowsky-Glahn, V. (2003). Composition and discrimination of sandstones: a statistical evaluation of different analytical methods. *Journal of Sedimentary Research*, *73*(1), 47-57.

von Eynatten, H., Tolosana-Delgado, R., Karius, V., Bachmann, K., & Caracciolo, L. (2016). Sediment generation in humid Mediterranean setting: Grain-size and source-rock control on sediment geochemistry and mineralogy (Sila Massif, Calabria). *Sedimentary geology*, *336*, 68-80.

Wagner, A., Lohmann, G., & Prange, M. (2011). Arctic river discharge trends since 7ka BP. *Global and Planetary Change*, *79*(1), 48-60.

Wang, J., Cota, G. F., & Comiso, J. C. (2005). Phytoplankton in the Beaufort and Chukchi Seas: distribution, dynamics, and environmental forcing. *Deep Sea Research Part II: Topical Studies in Oceanography*, *52*(24-26), 3355-3368.

Wheeler, J.O., Hoffman, P.F., Card, K.D., Davidson, A., Sanford, B.V., Okulitch, A.V., & Roest, W.R.(1996). Geological map of Canada Natural Resources Canada.

Wolfe, A. P. (1996). Spatial patterns of modern diatom distribution and multiple paleolimnological records from a small arctic lake on Baffin Island, Arctic Canada. *Canadian Journal of Botany*, *74*(3), 435-449.

Woodgate, R. A., Aagaard, K., Swift, J. H., Smethie, W. M., & Falkner, K. K. (2007). Atlantic water circulation over the Mendeleev Ridge and Chukchi Borderland from thermohaline intrusions and water mass properties. *Journal of Geophysical Research: Oceans*, *112*(C2).

Zabenskie, S., & Gajewski, K. (2007). Post-glacial climatic change on boothia peninsula, Nunavut, Canada. *Quaternary Research*, *68*(2), 261-270.

Zhang, D. (2000). *Flux de radio-isotopes à courte période dans les bassins marins marginaux de l'est canadien* (Doctoral dissertation, Ph. D. thesis, Université du Québec à Montréal, Montréal, Québec).

Zhang, X., He, J., Zhang, J., Polyakov, I., Gerdes, R., Inoue, J., & Wu, P. (2013). Enhanced poleward moisture transport and amplified northern high-latitude wetting trend. *Nature Climate Change*, *3*(1), 47.

Zhang, H., Amesbury, M. J., Ronkainen, T., Charman, D. J., Gallego-Sala, A. V., & VÄliranta, M. (2017). Testate amoeba as palaeohydrological indicators in the permafrost peatlands of north-east European Russia and Finnish Lapland. *Journal of Quaternary Science*, 32(7), 976-988.